EVALUATING THE BEHAVIOR OF AXIAL LAP STEEL CONNECTIONS MADE IN COMBINATION OF SLIP-CRITICAL BOLTS AND LONGITUDINAL FILLET WELDS UNDER DIRECT TENSION AND FATIGUE

By

CALEB W. BENNETT

Bachelor of Science in Civil Engineering

Oklahoma State University

Stillwater, Oklahoma

2019

Submitted to the Faculty of the
Graduate College of the
Oklahoma State University
in partial fulfillment of
the requirements for
the Degree of
MASTER OF SCIENCE
July, 2021

EVALUATING THE BEHAVIOR OF AXIAL LAP STEEL CONNECTIONS MADE IN COMBINATION OF SLIP-CRITICAL BOLTS AND LONGITUDINAL FILLET WELDS UNDER DIRECT TENSION AND FATIGUE

Thesis Approved:

Dr. Mohamed Soliman

Thesis Adviser

Dr. Bruce Russell

Dr. M. Tyler Ley

ACKNOWLEDGEMENTS

It has been a great honor to receive my education from Oklahoma State University. I always have, and always will, bleed orange.

I would like to thank my parents for supporting my journey to becoming a structural engineer. Without their help none of this would be possible. I would also like to thank my brother and grandmother, Jonan, you each have been great role models my entire life. I would also like to thank to my advisor Dr. Mohamed Soliman. He has constantly encouraged me over the last two years, and I have found a greater love for my work under his supervision. I give additional thanks to Dr. Bruce Russell and Dr. Tyler Ley, who both volunteered to serve on my committee and helped me significantly towards both my B.Sc. and M.Sc. degrees.

I also thank my fellow members of the research team: Omid Khandel, Ethan Stringer, Ligang Shen, and Mohammad Tamimi. Lastly, I am beyond thankful for the help of the undergraduate students who assisted our experiments in the Bert Cooper Lab: Adam Ross, Alex Rose, Connor Burgin, Ibrahim Al-Saggaf, James Gordon, Jeffrey Collier, Jordan Scott, Justin Hoppe, Rebecca Dempewolf, and Loyd Spaugy.

I would like to express my sincerest gratitude to the Oklahoma Center for the Advancement of Science and Technology (OCAST) (Project #AR18-37), American Institute of Steel Construction (AISC), W&W|AFCO Steel, and St. Louis Bolt and Screw for being generous sponsors in this study.

Name: CALEB W. BENNETT

Date of Degree: JULY, 2021

Title of Study: EVALUATING THE BEHAVIOR OF AXIAL LAP STEEL CONNECTIONS MADE IN COMBINATION OF SLIP-CRITICAL BOLTS AND LONGITUDINAL FILLET WELDS UNDER DIRECT TENSION AND FATIGUE

Major Field: CIVIL ENGINEERING

Abstract: Steel building and bridge connections have traditionally relied on either bolts or welds only to carry the required load from member to member. Due to the historical use of bolts or welds only, the combination of bolts and welds (referred to as the *combination connection*) is sparsely utilized in steel structures. However, it is apparent that knowing the behavior of these connections would extremely benefit existing infrastructure. In new construction, especially large structures, fit-up problems may occur and combining bolts and welds may be an economical solution to solve these problems. Unfortunately, neither research nor historical findings can provide the proper guidance as to how these connections can be treated in all situations. This study investigates the behavior of combination connections (a) in single shear configuration under direct tension monotonic and (b) under high cycle fatigue loading. The experimental study has great significance to both the steel building and bridge infrastructure. Large-scale experimental testing has been performed on 12 single shear joints in direct tension monotonic and 1 double shear joint under high-cycle fatigue. The single shear testing program evaluated the influence of weld to bolt ratio, weld location, and installation techniques when both slip-critical bolts and welds are used. An experimental fatigue test was conducted to aid in the categorization of the fatigue behavior of combination connection under AASHTO LRFD bridge design specifications. Accordingly, this experimental study supports the implementation of combination connections given the better characterization of their behavior under various loading conditions.

TABLE OF CONTENTS

LIST OF TABLES

Table Page

LIST OF FIGURES

Figure Page

CHAPTER I

1 INTRODUCTION

1.1 OVERVIEW

In typical steel construction, connections are traditionally made up of either bolts or welds alone. The use of bolts and welds in combination (referred to as a *combination connection* in this thesis document) is rarely used in steel structures. However, the use of combination connections can have significant benefits to steel infrastructure. The combination connection is an economical solution for retrofitting existing structures to increase strength, relieve unanticipated fit-up problems, and increase the load-carrying capacity of a connection during the construction phase if design loads are increased. However, past research studies on evaluating the load-deformation behavior of the individual fasteners (i.e., bolts and welds) showed that they do not reach their ultimate capacity at the same deformation level. As a result, the load-deformation behavior and the ultimate capacity of a connection with a combination of bolts and welds in a shared load system cannot be easily characterized. Previous studies in literature [9-11,22-25], as well as recent experimental programs at Oklahoma State University [22] have been conducted to investigate the behavior of double shear splice connection with bolts and fillet welds in combination. In this thesis, the behavior of single shear axial-lap

connections utilizing slip-critical bolts and longitudinal fillet welds is investigated through experimental and numerical finite element analysis. A general layout of these connections is shown in Figure 1.1.

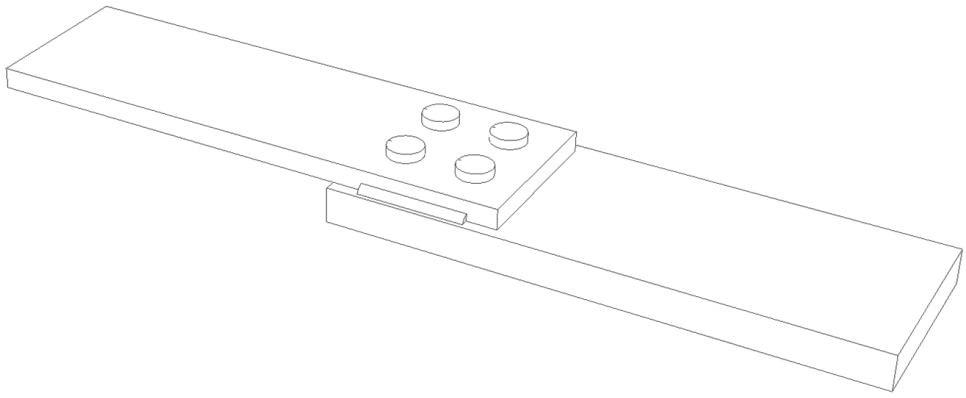

Figure 1.1: Model of Single Shear Combination Connection

The load-deformation behavior of the combination connections was recorded during the large-scale experiments and used to develop a better understanding of the influence of key test variables on the capacity of these connections. Test variables for the single shear axial-lap splices under direct tension include weld to bolt strength ratio, connecting elements installation sequence, and the weld location compared to the center of the bolted connection. Finite element models are constructed and verified using the results of the experimental testing and a parametric study is conducted to evaluate the influence of plate thickness and weld length on the behavior of the connections. Lastly, the slip capacity and ultimate capacity are compared with the prediction method outlined in the

2016 Specification for Structural Steel Buildings [2] and the As-Built prediction method from previous testing of double shear combination connections [11,22].

If the combination connection is to be utilized in structures that experience fluctuations in loading (e.g., bridges under traffic loads), further testing must be performed to characterize the fatigue behavior. Previous studies have been performed to quantify the fatigue life of bolted or welded only connections under constant amplitude loading. However, fatigue testing conducted on connections with bolts and welds in combination is very rare in literature. The results of such testing are essential to classify the fatigue life of these connections based on the detail categories outlined in the *AASHTO LRFD Bridge Design Specifications* [8]. To provide better guidance in such a scenario, a brief experimental investigation into the performance of double shear axial-lap steel connections (see Figure 1.2) under high-cycle fatigue loading has been performed. The stiffness and crack propagation over the lifetime of the combination connection are investigated. The fatigue life of the tested connection is also compared to the AASHTO S-N curves to provide better guidance over the fatigue response of a typical combination joint detail.

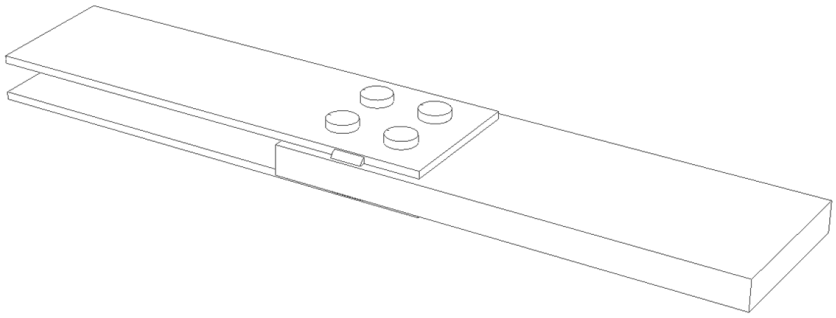

Figure 1.2: Double Shear Combination Connection

1.2 THESIS SCOPE AND OBJECTIVES

The main goal of this thesis is to characterize the behavior of connections using pretensioned bolts and longitudinal fillet welds in a shared load system. The primary objectives and scope of this research study are:

1. Review previous research on the ultimate capacity, load-deformation response, and fatigue life of bolted, welded, and combination connections with a single and double shear configuration.
2. Construct an experimental test matrix to evaluate the effect of key factors affecting the behavior of the single shear axial lap splice connections. These include weld/bolt strength ratio, installation sequence, and weld location.

3. Quantify the capacity of bolted and welded combination connections in a single shear configuration using experimental and numerical analysis. In additional to the large-scale tests, finite element modeling is utilized to develop a deeper understanding of the behavior of these connections and the experimental results are compared to current provisions outlined by the AISC.
4. Perform experimental testing to evaluate the fatigue life of double shear axial lap connections with pretensioned bolts and longitudinal fillet welds in combination.

1.3 THESIS ORGANIZATION

This thesis is organized by the following chapters:

Chapter 1 provides an introduction of the research work conducted in this thesis. The objectives of this study and the organization of this document are also explained.

Chapter 2 provides a literature review and discussion on previous studies conducted on steel connections with slip-critical bolts and welds. Experimental work performed to quantify the capacity of the connection under direct tension is discussed. Studies on quantifying the fatigue life of the bolted-only, welded-only, and combination connections under constant amplitude fatigue loading are also reviewed.

Chapter 3 describes the experimental methods used to conduce direct tension and fatigue testing. This includes description of the existing load frame at the Bert Cooper Engineering Laboratory at Oklahoma State University, the test specimens, test matrix, data acquisition methods, and the testing procedures.

Chapter 4 presents the test results for the 12 direct tension and one fatigue loaded tests. This includes the load-deformation behavior of the direct tension test, and the behavior of the fatigue specimen over its life cycle.

Chapter 5 evaluates the results of the experimental investigation. This includes a discussion of the effects of both weld location and connection assembly sequence. The investigation of the assembly sequence covers connections in which the bolts were pretensioned before placing the welds and others that were welded before bolt installation. Finite element modelling of the tested connections is also discussed in this chapter. Finally, a discussion on the fatigue behavior of the tested connection is included.

Chapter 6 presents the final conclusions of the experimental testing and evaluation. Additionally, recommendations for future research of related steel connections is provided.

CHAPTER II

2 LITERATURE REVIEW

2.1 INTRODUCTION

Historically, large scale experimental results have shown that the ultimate capacity of single shear lap joints is approximately equal to half that of the double shear lap joint [12]. However, due to the inherent eccentricity in the load transfer mechanism of the single shear configuration, the effects of secondary bending may induce significant change in the load-deformation behavior compared to a concentrically loaded double shear joint. In this chapter, a review of literature has been performed to identify the key factors that affect the behavior of single shear joints with both bolts and welds utilized in the same load sharing system. Although no specific work has been found in literature on the single shear joint with bolts and welds in combination, studies on the combined double shear joint and single shear joints with high-strength bolts are reviewed.

Furthermore, little experimentation has been performed to evaluate the fatigue behavior of double shear lap spice connections with bolts and welds in combination. In this chapter, previous research on the fatigue behavior of similar double shear lap splice connections using bolts and welds as individual fasteners, and in combination, will be reviewed.

2.2 STRENGTH OF INDIVIDUAL FASTENERS

2.2.1 Slip-Critical Bolt Strength

Pretensioned high strength bolts are the primary fastening component used to construct a slip-critical joint. In a typical slip-critical joint, the load will be transmitted through the frictional forces acting on the surface of the connected plates (i.e., faying surface). The maximum slip capacity of these joints is reached when the frictional resistance of the joints is surpassed. When this load is exceeded, slip between the plates will occur and eventually the bolt bearing on the connection components will occur.

When load is applied parallel to the slip-critical joint, the slip load can be determined as:

$$P_{slip} = k_s m \sum_{i=1}^{n} T_i \qquad \text{Eq. 1 [1]}$$

where, P_{slip} = slip load, k_s= Slip Coefficient

m= Number of Slip Planes

$\sum_{i=1}^{n} T_i$ = Sum of individual bolt pretension force

When the pretension in each bolt of the connection is assumed to be equal this equation reduces to:

$$P_{slip} = k_s m n T_i \qquad \text{Eq. 2 [1]}$$

n= Number of bolts

The guidance on design of slip-critical connections has remained mostly unchanged since the introduction of high strength bolts. From 1987 to 2005, changes to Equation (1)

above included the addition of a strength reduction factor of 15% in connections with oversized holes, 30% for long slotted holes perpendicular to the load, and 40% for long slotted holes parallel to the applied load [2]. Additional changes were made during this time to accommodate LRFD code provisions.

The 2005 AISC *Specification* [2] increased the reliability levels for the design of slip-critical connections. To accomplish this, the 2005 AISC *Specification* design procedure was calibrated to resist slip at factored loads if the slip at service loads could reduce the ability of the structure to support factored loads [2]. This new procedure arose from the increase in popularity of slip-critical connections in construction.

The current design procedure used for calculating the capacity of slip-critical connections was first used in the 2010 AISC *Specification*. The 2010 provisions for slip-critical bolts were primarily a result of research projects conducted by [37,38,39] . Investigation of the performance characteristics of Class A faying surfaces, oversized holes, loss of pretensioning, tightening with the Turn-of-Nut (ToN) method, shear/bearing strength, and the influence of fillers in slip-critical joints were all variables in the three research projects prior to 2010. As a result, the 2010 AISC *Specification* provisions were based on the following findings:

a) Class A faying surfaces supports the use of a mean friction coefficient $\mu = 0.31$. However, the use of $\mu = 0.30$ was selected to achiever more consistent reliability.
b) When multiple filler plates are used, a new factor, h_f, was needed to achieve a better prediction of the nominal slip resistance.

Therefore, the nominal slip resistance of a slip-critical connection according to the 2010 AISC *Specification* was determined as:

$$R_n = \mu D_u h_f T_b n_s \qquad \text{Eq. 3 (AISC J3-4) [2]}$$

h_f = Factor for fillers

D_u = 1.13, a multiplier that reflects the ratio of the mean installed bolt pretension to the specified minimum pretension.

T_b = Minimum pretension

n_s = Number of slip planes required to permit the connection to slip

μ = mean slip coefficient for Class A or B surfaces

2.2.2 Longitudinal Fillet Weld Strength

In 1928, the American Welding Society (AWS) Code for Fusion Welding and Gas Cutting in Building Construction [30] was first published. At that time, a working shear stress of 11.3 ksi was permitted on the throat of a fillet weld [3]. As a result of a testing program in 1940 [4] the allowable stress of fillet welds was shown to be 20% higher when installed in accordance to the Code [4]. Therefore, the allowable shear stress was raised to 13.6 ksi [4]. In 1969, a study by Higgins and Preece [5] concluded that a 30% increase in the allowable shear stress appeared fully justifiable. Additionally, the study [5] covered steels having yield strength as high as 100 ksi and weld electrodes of comparable strength. The findings in [5] made it convenient for the implementation of higher strength steels and electrodes in steel construction.

Eq. 4 below, used in the current edition of the AISC *Steel Construction Manual* [7], quantifies the nominal shear resistance of fillet welds as 60% of the minimum tensile strength of the weld material. It is also assumed the weld is in pure shear and that the distortion energy theory is the approximate condition of the plastic flow in the material [6]. This equation, proposed by Fisher et al. [6], can be implemented for the calculation of available shear strength of a fillet weld with length less than or equal to 100 times the weld size.

$$R_n = F_{nw}A_{we} \qquad \text{Eq. 4 [6]}$$

$$R_n = 0.6F_{EXX}A_{we} \qquad \text{Eq. 5 [6]}$$

$$R_n = 0.6F_{EXX}\left(\frac{\sqrt{2}}{2}\right)\left(\frac{D}{16}\right)l \qquad \text{Eq. 6 (AISC 8-1) [7]}$$

F_{EXX} = Filler metal classification strength, ksi

D = Weld size in sixteenths of an inch

l = *Length of weld, in*

2.3 FATIGUE BEHAVIOR OF CONNECTIONS WITH INDIVIDUAL FASTENERS

2.3.1 Slip-Critical Bolted Connections

Fatigue life estimation of slip-critical bolted connection can be performed using the stress-life (i.e., *S-N*) approach outlined by the *AASHTO LRFD Bridge Design Specifications*. To better understand the performance of combination connections under fatigue loading, the fatigue performance of each individual fastener system should be

thoroughly investigated. Many research programs have been conducted in literature to better characterize fatigue life of slip-critical bolted connections. The current AASHTO design provisions [8] list slip-critical bolted connections with drilled holes to follow detail Category B. Figure 2.1 displays the fatigue detail category for a slip-critical connection as described in Table 6.6.1.2.3-1 of *AASHTO LRFD Bridge Design Specifications* [8].

Table 2.1: Fatigue detail of a slip-critical connection

[adapted from *AASHTO LRFD Bridge Design Specifications Table 6.6.1.2.3-1: Detail 2.1* [8]]

	Description	**Category**	**Constant A (ksi^3)**	**Threshold $(\Delta F)_{TH}$ ksi**	**Potential Crack Initiation Point**
Bolted-Only (Slip-Critical Bolts)	2.1 Base metal at the gross section of high-strength bolted joints designed as slip-critical connections with pre-tensioned high-strength bolts installed in holes drilled full size or subpunched and reamed to size -- e.g., bolted flange and web splices and bolted stiffeners.	B	120×10^8	16	Through the gross section near the hole

2.3.2 Fatigue Life of Connections with Longitudinal Fillet Welds

The AASHTO LRFD Bridge Design Specifications provide fatigue details for welded joints in Section 3 of Table 6.6.1.2.3-1 [8]. For the configuration of concern in this thesis, shown in Figure 2.2, since no similar details can be found in AASHTO Table 6.6.1.2.3-1, Detail 3.5 will be considered. This detail represents the termination of a cover plate

connected to the flange of a member by longitudinal fillet welds. Figure 2.2 displays the S-N parameters of this details presented in [8]. .

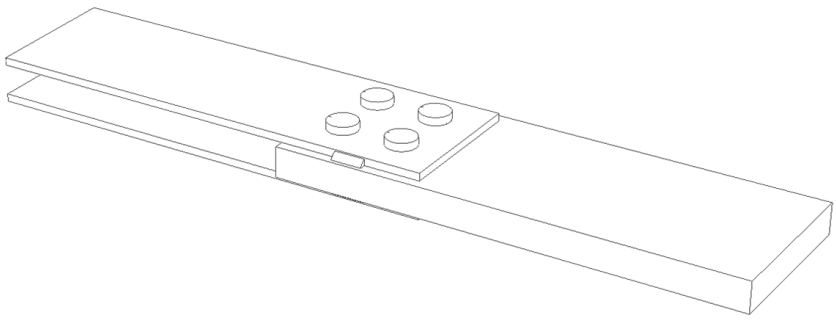

Figure 2.1: Configuration of Double Shear Combination Connection used in Fatigue Testing

Table 2.2: Fatigue detail of a welded cover plate without welds across the ends

[adapted from *LRFD Bridge Design Specifications Table 6.6.1.2.3-1: Detail 3.5* [8]]

	Description	**Category**	**Constant A (ksi^3)**	**Threshold $(\Delta F)_{TH}$ ksi**	**Potential Crack Initiation Point**
Welded-Only	3.5 Base metal at the termination of partial length welded cover plates having square or tapered ends that are narrower than the flange, with or without welds across the ends, or cover plates that are wider than the flange with welds across the ends:			In the flange at the toe of the end weld or in the flange at the	At end of weld
	Flange Thickness ≤ 0.8 in	E	11×10^8	4.5	
	Flange Thickness > 0.8 in	E'	3.9×10^8	2.6	

2.4 CONNECTIONS WITH BOLTS AND WELDS IN COMBINATION

Several experimental research programs have been performed to characterize the behavior of double shear axial lap splice connection with bolts and welds used in a shared load system (e.g., [9,10,23]). However, no experimental work on the single shear configuration of the axial lap combination connections has been reported in literature. Historically, for slip-critical bolted- or welded-only connections, the capacity of the single shear configuration has been determined as half the capacity of the double shear configuration of the same connection [12]. Among the notable studies that have investigated the behavior of the load sharing system of double shear connections with bolts and welds in combination are Holtz and Kulak (1970) [9], Jarosch and Bowman (1986) [10], Kulak and Grondin (2003) [23]. These studies mainly focused on weld orientation (longitudinal and transverse) and concluded that longitudinal fillet welds are more efficient in combination with pretensioned bolts. However, the effect of other key parameters that may affect the behavior of these connections has not been fully characterized.

Recently, an experimental research program has been competed at Oklahoma State University to fully characterize the behavior of double shear axial-lap connections with slip-critical bolts and welds in combination [11]. The purpose of the experimental program in [11] was to explore the influences of key variables in combination connections that were not clearly outlined or understood in previous work. Variable of the testing program included: bolt pattern, bolt grade, bolt size, tensioning technique, faying surface class, and weld/bolt strength ratio. The experimental program consisted of 75 double shear axial-lap connection specimens which were tested at the Bert Cooper

Engineering Lab in Stillwater, Oklahoma. The test results of 75 large-scale experimental test displayed an average capacity that was beyond 42-79% the predicted capacity by AISC [11]. This was attributed to the higher capacities of connecting elements (i.e., bolt pretension force or weld ultimate capacity) compared to the nominal design values. Additionally, the investigation in [11] quantified the difference in the load-deformation behavior induced by the faying surface class. Connections with Class A faying surface displayed an increase in capacity beyond the slip load; however, connections with Class B surfaces have high initial stiffness but would lose the slip capacity after the ultimate slip load [11]. Test data was further investigated to judge the accuracy of the AISC prediction model based on the As-Built characteristics of the connection. The As-Built characteristics included the measured pretension force, actual weld dimensions, and ultimate weld shear strength estimated from welded-only tests. This prediction was denoted the As-Built capacity [11]. The equation to predict the capacity of slip-critical bolts remained similar to the current provision by AISC; however, values of the parameters were updated based on test data. The As-Built capacity of slip-critical bolts is computed as

$$R_b = \mu h_f n_s T_B \qquad \text{Eq. 7 [11]}$$

$\mu =$ experimental slip coefficient for Class A or B surfaces (μ = 0.457 for Class A (2×2); μ = 0.339 for Class A (2×3); μ = 0.535 for Class B) [22].

$h_f =$ 1.0; factor for fillers (no fillers)

$n_s =$ number of slip planes

$T_B =$ fastener tension

The As-Built capacity of fillet welds can be determined using the following equation.

$$R_w = \tau t_e l \qquad \text{Eq. 8 [11]}$$

$\tau =$ weld shear stress

$t_e = \frac{ab}{\sqrt{a^2+b^2}}$; the shortest distance of the weld from the root to the face of the weld, where a and b are the measured legs of the fillet weld. This accommodates unequal leg sizes [27].

$l =$ weld length, in

Then the As-Built capacity of the combination connection is

$$R_n = R_b + R_w \qquad \text{Eq.9 [11]}$$

2.4.1 AISC Specification for Structural Steel Buildings (2017)

The use of steel connections with bolts and welds in combination is currently permitted under Section J1.8 of the *Specification for Structural Steel Buildings.* This section states the shared load system between bolts and welds may only be used in shear connections on a common faying surface where strain compatibility between the bolts and welds is considered. The specification permits the strength, φR_n and R_n/Ω, of the joint combining high-strength bolts and longitudinal fillet welds as the summation of the nominal slip resistance of the high strength bolts and nominal weld strength. The nominal slip resistance, R_n, for the high strength bolts is determined by equation J3-4. The nominal weld strength, R_n, is determined by Section J2.4. This case is true only when the following cases are applied in the design of the combination connection [2]:

a) $\phi = 0.75\ (LRFD);\ \Omega = 2.00\ (ASD)$ for the combined joint.
b) When the high-strength bolts are pretensioned according to the requirements of Table J3.1 or Table J3.1M, using the turn-of-nut method, the longitudinal fillet

welds shall have an available strength of not less than 50% of the required strength of the connection.

c) When the high-strength bolts are pretensioned according to the requirements of Table J3.1 or Table J3.1M, using any method other than the turn-of-nut method, the longitudinal fillet welds shall have and available strength of not less than 70% of the required strength of the connection.

d) The high-strength bolts shall have an available strength of not less than 33% of the required strength of the connection.

It should also be noted that no requirement is present to restrict the design capacity of the combination joint as either the strength of the bolts alone or the strength of the welds alone.

2.5 PREVIOUS TENSILE TEST OF SINGLE SHEAR CONNECTIONS WITH SNUG TIGHT AND SLIP-CRITICAL BOLTS

Although very little experimental research has been performed on the single shear axial-lap splice steel connections with bolts and welds used in combination, experimental work exists for the single shear configuration using high strength bolts as individual fasteners. The following gives a summary of 4 of these studies on bolted only lap splice connections with a single shear plane.

2.5.1 Bendigo, Fisher, and Rumpf (1962) [12]

Early testing of bolted lap joints was performed by Bendigo, Fisher and Rumpf at Lehigh University in 1962. The goal of this testing was to verify the behavior of structural joints using ASTM A325 bolts prior to the release of the *1960 specification for structural*

joints. The large-scale experimentation consisted of four 1” thick test specimens and 2 lines of 7/8” diameter A325 bolts with two to ten bolts per line. With the realization that bending would occur, an external bracing system was installed and adjusted during load application in order to keep the joint plumb. It was noted that although the external bracing was used, not all bending effects were eliminated. At the end of four experimental tests, the researchers concluded the ultimate capacity of the connection is approximately one half that of the double shear joint [12]. The study noted the difference as a function of the number of shear planes [12].

2.5.2 Shoukrey and Haisch (1970) [13]

In 1970, Shoulkrey and Haisch [13] carried out and experimental program to determine the effects of bolt hole size on the capacity of single and double lap shear connections. A total of 18 lap splice connections were tested with ¾" and 7/8” ASTM A325 bolts placed in holes oversized by 1/16”, 1/8” and 3/16”. It was observed in testing that most damage to the mill scale surface was confined to the area around the bolts [13]. The results of testing concluded that a hole may be oversized to 3/16” without a significant impact on the slip performance of the connection [13]. It was also noted that the ultimate shear stress of the single shear lap joint is less than the double shear lap joint [13]. This behavior was attributed to the moment induced in the lap joint by load eccentricity.

2.5.3 Heistermann (2011) [14]

With the increased demand of renewable energy, Heistermann [14] analyzed typical construction practices associated with wind towers in order to reduce the costs. In this

study, the behavior of pretensioned bolts in single and double shear slip-critical connections was quantified experimentally and investigated in a finite element study. Once calibrated, the finite element model constructed using Abaqus software [31was in good agreement with the experimental data. Finite element modeling is crucial to properly understand the behavior of tested components

By using the calibrated finite element model, Heistermann evaluated the slip resistance of the single shear connection with different sizes of gaps between the connected plates to access levels of assembling tolerances. A reduction of 10.7% at a slip level of 0.15 mm (0.006 in) was found when comparing the load-deformation response of connection plates with no gap, a 1 mm gap, 2 mm gap and 3 mm gap present[14]. Therefore, assembling tolerances have a negative effect on the total resistance of the connection. Additionally, for the single shear connection it was found the connection could withstand higher loads beyond a slip of 0.15 mm [14]. It was noted that a clear plateau in the data could not be obtained due to the secondary bending effects in the single shear configuration.

Another comparison was made in the results by Heistermann regarding the differences in single shear and double shear connections. The nominal stress in both configurations were approximately the same at a slip level of 0.15 mm, however, noticeable differences were observed in the failure mechanisms of each configuration. The double shear configuration ultimate resistance was found to occur prior to the defined slip criterion of 0.15 mm because of its symmetric configuration. However, the ultimate resistance of the single shear configuration extended beyond the failure criterion due to its asymmetric configuration, which allows for secondary bending [14].

2.6 PREVIOUS FATIGUE TEST OF DOUBLE SHEAR CONNECTIONS

The majority of previous research in literature has focused on studying the fatigue life of steel connections utilizing high strength bolts and welds as individual fasteners. A study by Bowman, Fu, Zhou, Connor and Godbole (2012) [20] was conducted to characterize the fatigue life of connections with rivets and tack welds in combination. The following section will discuss studies focusing on estimating the fatigue life of bolted-only, welded-only and combination joints.

2.6.1 P. B. Keating and J.W. Fisher (1986) [16]

Several National Cooperative Highway Research Program (NCHRP) studies (e.g., [32-34]) focused on evaluating the fatigue behavior of welded joints. In 1986, *NCHRP Report 286* [16] was published by Keating and Fisher to review previous fatigue studies and the guidelines created to design welded joints for fatigue. At the time of publishing the report, many of the AASHTO fatigue guidelines were based on the test information collected from 1966 to 1972. Since that time, additional work had been performed on the fatigue strength of welded details both in the United States and abroad. The objective of the report was not to define new approaches to rehabilitation but it attempted to define a lower bound fatigue resistance for welded details.

In constructing this review, Keating and Fisher revised the AASHTO curves to a more uniform curve with a slope of -3.0 [16]. It was noted in previous studies of welded attachments that all fatigue cracks were found to initiate at some geometrical discontinuity and grew perpendicular to the applied stress [16]. Investigations also

showed that the stress range was the most important factor in determining the fatigue life. A regression analysis showed the stress range – fatigue life behavior to be log-log, with a constant slope. Therefore, the S-N curves are defined by

$$log\ N = log\ A - B * log\ S_r \qquad \text{Eq. 11 [16]}$$

where $logA$ is the log-N-axis intercept of the log S-N curve, N is the number of cycles to failure, B is the slope of the curve, and $S_r$is the stress range.

In this review, welded-only cover plate details were determined to surpass Category E and E' depending on the length of the weld and thickness of the plate.

2.6.2 J.D. Brown, D.J. Lubitz, Y.C. Cekov, K.H. Frank, and P.B. Keating (2007)

In 2007, direct tension monotonic and fatigue tests were performed and reported by Brown, Lubitz, Cekov, Frank and Keating. In this research program, fatigue testing was performed on connections with bolts in both bearing and slip-critical configurations. One of the goals was to determine the influences of hole making procedure (i.e., punched or drilled) on the fatigue life and ultimate tensile capacity of connections. It was concluded the effect of hole making was reduced for both the tensile capacity and fatigue life when connections were constructed as slip-critical using pretensioned bolts [18]. This also reaffirmed the conclusions made by Huhn and Valtinat [19], who found the use of pretensioned bolts to negate the effects of punching connected plates[19].

In this experimental program, a total of 12 connections were tested under constant amplitude fatigue loading. Each specimen consisted of a 6 in. wide, ½ in. thick A572 Grade 50 steel plate with 5/16 in. diameter holes. The stress ranges of the connections

were determined based on the gross cross-sectional area. Of the 12 tests, 6 were conducted using pretensioned bolts. The results of the testing with pretensioned bolts showed that the connection had a greater fatigue life than required by Category B, regardless of how the holes were fabricated [18].

2.6.3 M.D. Bowman, G. Fu, Y.E. Zhou, R.J. Connor and A.A. Godbole (2012) [20]

The testing program discussed in the *National Cooperative Highway Research Program (NCHRP) Report 721 [20]* was performed to identify the fatigue detail category riveted connections with tack welds. Experimental testing was performed on a total of 17 connection specimens. Each specimen consisted of a double shear axial-lap connection with welds and pretensioned bolts. The pretensioned bolts were used in place of rivets that are common on older bridge structures. These bolts were pretensioned using the turn-of-nut method (ToN) to exceed the minimum required pretension of 39 kips. The net section was used in testing to calculate the stress because it is used frequently in riveted connections [20]. The results of experimental testing lied clearly above the Category D AASHTO S-N line and near the Category C mean curve [20].In each test, cracks were found to propagate from weld toe to the adjacent bolt hole. As this was the case for all connections, the failure criterion was met when the crack propagated from the edge of the plate to the adjacent bolt hole, or a test runout occurred. Figure 2.7 displays a typical crack that occurred in the test specimens. It was noted in some tests that cracks would start growing at multiple locations before reaching the adjacent bolt hole. However, the test was stopped once a crack had reached the adjacent bolt hole or the test was deemed a runout.

Additionally, a finite element investigation was formulated to observe the stress concentrations in the tack welds. It was concluded that the location of the crack was consistent with the location of maximum stress concentration predicted by the finite element model [20].

2.6.4 AASHTO LRFD Bridge Design Specifications, 7th Edition (2014)

Currently no fatigue classification is assigned for connections utilizing bolts and welds in combination. However, for connections that undergo load or distortion induced fatigue *Section 6.6* of the *AASHTO LRFD Bridge Design Specifications* should be followed for designing bridge components. Under this provision, all fatigue details that undergo load induced fatigue, a stress range produced by the live loads on the structure should satisfy [8]:

$$\gamma(\Delta f) \leq (\Delta F)_n \qquad \text{Eq. 12 [8]}$$

γ = Load factor specified in Table 3.4.1-1 for the fatigue load combination

(Δf) = Force effect, live load stress range due to the passage of the fatigue load as specified in Article 3.6.1.4 (ksi)

$(\Delta F)_n = nominal\ fatigue\ resistance\ as\ specified\ in\ Article$ 6.6.1.2.5 (ksi) = Nominal fatigue resistance as specified in Article 6.6.1.2.5 (ksi)fatigue resistance of a structural detail should be taken as

- For the Fatigue I load combination and infinite life:

$$(\Delta F)_n = (\Delta F)_{TH} \qquad \text{Eq. 13}$$

- For the Fatigue II load combination and finite life:

$$(\Delta F)_n = \left(\frac{A}{N}\right)^{\frac{1}{3}} \qquad \text{Eq. 14}$$

Where, $N = (365)(75)n(ADTT)_{SL}$

A = Constant taken from Table 6.6.1.2.5-1 (ksi^{-3}) [8]

n = Number of stress range cycles per truck passage taken from Table 6.6.1.2.5-2 [8]

$(ADTT)_{SL}$ = Single-lane ADTT as specified in Article 3.6.1.4 [8]

$(\Delta F)_{TH} = constant - amplitude\ fatigue\ threshold\ taken\ from\ Table$ 6.6.1.2.5 − 3 (ksi) = Constant-amplitude fatigue threshold taken from Table 6.6.1.2.5-3 (ksi) [8]

When plate elements are connected with a pair of fillet weld or partial joint penetration groove welds on opposite sides of the plate the nominal fatigue resistance should be taken as:

$$(\Delta F)_n = (\Delta F)_n{}^c \left(\frac{0.65 - 0.59\left(\frac{2a}{t_p}\right) + 0.72\left(\frac{w}{t_p}\right)}{t_p{}^{0.167}}\right) \leq (\Delta F)_n{}^c \qquad \text{Eq. 75}$$

where, $(\Delta F)_n{}^c = nominal\ fatigue\ resistance\ for\ Detail\ Category\ C\ (ksi)$ = Nominal fatigue resistance for Detail Category C (ksi)

$2a$ = Length of the non-welded root face in the direction of the thickness of the loaded plate (in). For fillet welded connections, the quantity $\left(\frac{2a}{t_p}\right)$ shall be taken equal to 1.0

$t_p = thickness\ of\ loaded\ plate\ (in.)$ = Thickness of loaded plate (in)

w = Leg size of the reinforcement or contour fillet, if any, in the direction of the thickness of the loaded plate (in)

The current AASHTO provisions include 8 sections that contain specific connection details. The two details of concern in this thesis, as mentioned in Section 2.3 above, are details 2.1 and 3.5 of Table 6.6.1.2.3-1 [8]. Therefore, the bolted-only case would be classified as Category B and the welded-only case would be classified as Category E. Figure 2.8 shows the constants for respective detail categories [8].

Table 2.3: AASHTO Fatigue Constant, A (ksi^3)

[Adapted from Table 6.6.1.2.5-1 -- Detail Category Constant, A of AASHTO LRFD Bridge Design Specifications]

Detail Category	**Constant, A times 10^8 (ksi^3)**
A	250
B	120
B'	61
C	44
C'	44
D	22
E	11
E'	3.9
M 164 (A325) Bolts in Axial Tension	17.1
M 253 (A490) Bolts in Axial Tension	31.5

Now, if the stress range of the connection is known, then a lower bound limit of the number of cycles to failure for a specific detail category can be determined.

2.7 NEW EXPERIMENTAL WORK

The work provided in this thesis was conducted to spread a greater depth of knowledge on the behavior of combination connections. In particular, the research reported in this thesis focuses on the load-deformation behavior of single shear axial-lap splice combination connections and fatigue life of double shear axial-lap splice combination connections.

Previous research on bolted-only single shear joints and double shear splices with slip-critical bolts and welds has been reviewed to supplement the single shear experimental testing. However, as indicated above, no previous experimental work was found in regards to the single shear joints with bolts and welds in combination. The information gathered in this chapter was used to in support of the research work conducted herein. Additionally, no research has been conducted previously to investigate the effect of weld location with respect to the bolts and the connection assembly sequence. A finite element model will be established for the combination connection and its outcomes will be compared to the single shear experimental results. Furthermore, a parametric study will be performed using the finite element model to better understand the effects of plate thickness and weld length on the behavior of the connection.

Another experimental testing program will be conducted on double shear axial-lap joints. Previous findings on the behavior of bolts and welds as individual fasteners have shown that bolts perform as Category B and welds may perform closer to Category E. Note that the current AASHTO specifications do not offer a detail category for the exact

configuration tested. Accordingly, it was of interest to evaluate the fatigue life of these combination connections to identify their appropriate detail category.

CHAPTER III

3 EXPERIMENTAL METHODS

3.1 INTRODUCTION

This chapter describes the experimental test methods used to complete both the direct tension monotonic and fatigue experimental testing. The following discussion covers the design of the experimental test specimens, testing matrix, test frame characteristics, instrumentation plan, and the testing procedure.

3.2 TEST SPECIMENS

3.2.1 Monotonic Tension Test Single Shear Specimens

The tested connection specimens for the single shear monotonic tension testing consisted of a single splice plate, upper grip plate and lower grip plate. Each connection was made up of an ASTM A572 grade 50 steel material. Each test specimen consists of three main components: the tested connection, test grip, and anchorage zone, which can be observed in Figure 3.1. It should be noted that the tested region of the specimen is only the hatched area of Figure 3.1(b). The thickness of all splice plates is 7/8" and the faying surface is Class B for all specimens. The steel surface had been blast cleaned by the fabricator to remove all mill scale and rust to conform with SSPC – SP 6 as required by the AISC [2] for Class B faying surfaces.

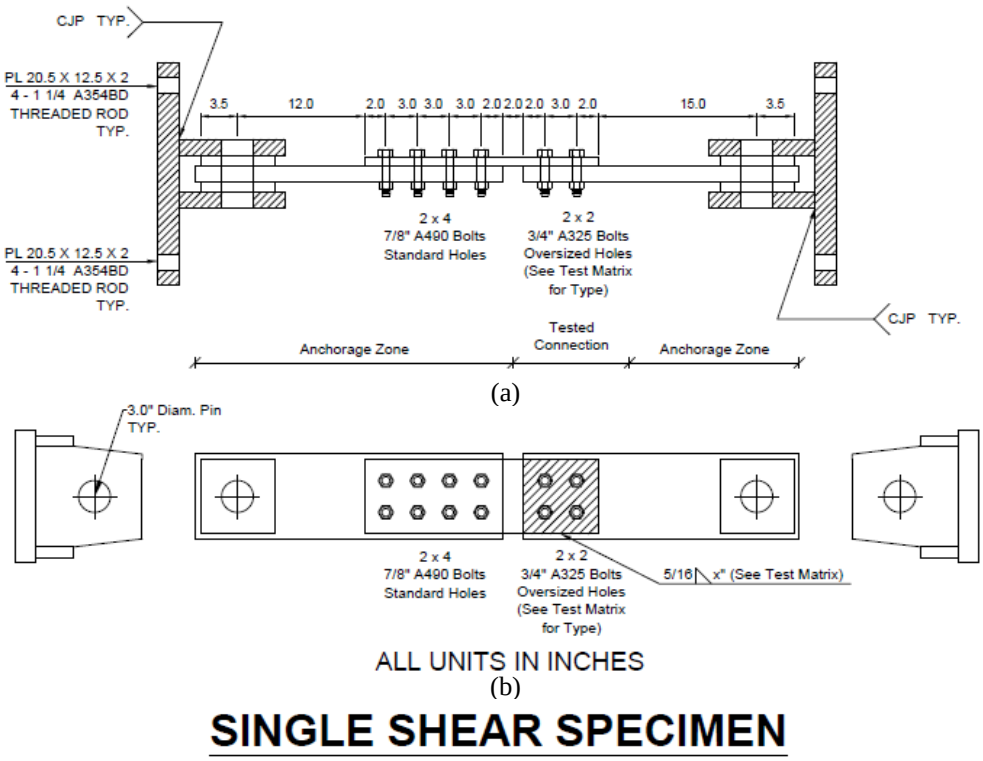

Figure 3.1: Single Shear Test Specimen (a) Elevation view (b) Plan view

3.2.2 Fatigue Test Specimens

A double shear lap splice specimen was used for the fatigue test included in this thesis. To achieve a realistic stress level in the plates during the tests, the test specimen splice plate was reduced to 3/8" thick with a class A faying surface. Figure 3.2 shows a typical fatigue connection specimen. The hatched section in Figure 3.2(b) is the tested connection region. Since field splice connections are expected to be symmetric, the test region was expanded in these specimens to include both sides of the splice gap as shown in Figure 3.2. As shown in the figure, each combination connection consists of four bolts

and four fillet weld lines. Since crack were expected to initiate at weld toes, each connection has eight possible crack initiation points that were closely monitored during the tests.

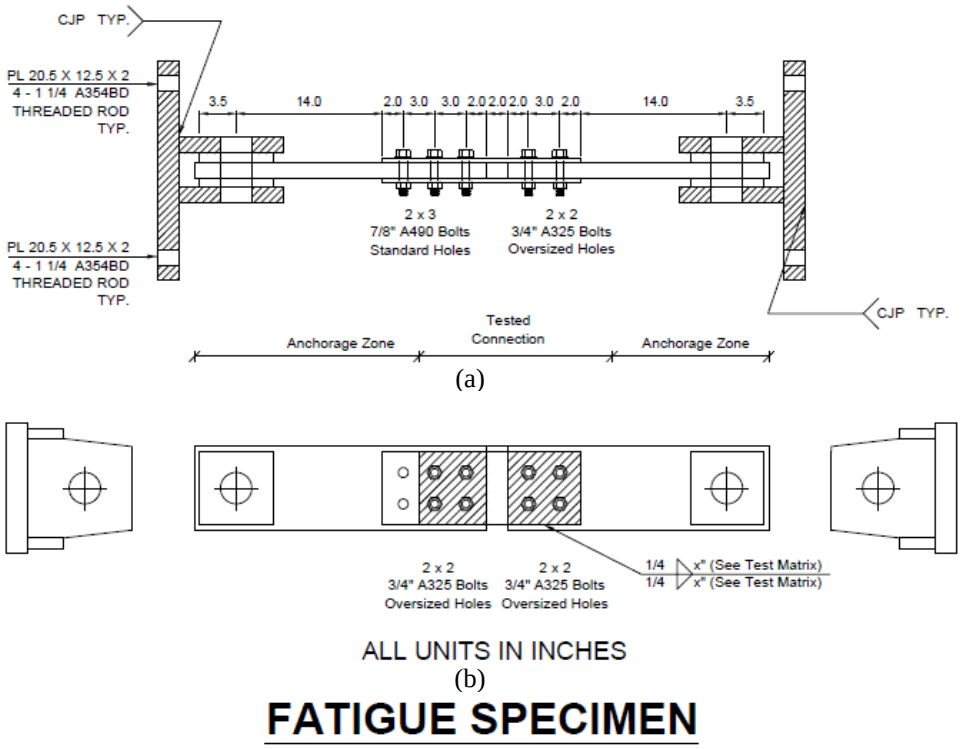

Figure 3.2: Fatigue Test Specimen (a) Elevation View (b) Plan View

3.3 TEST MATRIX

3.3.1 Single Shear Monotonic Tension Tests

The testing matrix for single shear specimens under direct tension monotonic loading is provided in Table 3.1. The testing matrix consist of a single bolted-only connection and welded-only connection test followed by the testing of 10 combination connections.

These combination tests were designed to characterize the effect of weld/bolt ratio, weld location, and specimen installation sequence. All bolts were installed using the turn of nut method conforming to the requirements of [28]. All connections in the test matrix used Class B faying surface and ASTM A325 3/4-in diameter bolts.

Table 3.1: Single Shear Direct Tension Testing Matrix

	Test No	Series	Weld Location	Assembly Sequence (Pretension before/after Weld)	Weld/Bolt Ratio	Weld Geometry (Size x Length) (in)
Bolted-Only	1	A	Bolt C.G.	---	---	---
Welded-Only	2	A	Bolt C.G.	---	---	5/16 x 4.5
Bolted & Welded	3	A	Bolt C.G.	before	0.9	5/16 x 3
		B	Bolt C.G.	before	0.9	5/16 x 3
	4	A	Bolt C.G.	before	1.33	5/16 x 4.5
		B	Bolt C.G.	before	1.33	5/16 x 4.5
	5	A	Above Bolt C.G.	before	1.33	5/16 x 4.5
		B	Above Bolt C.G.	before	1.33	5/16 x 4.5
	6	A	Below Bolt C.G.	before	1.33	5/16 x 4.5
		B	Below Bolt C.G.	before	1.33	5/16 x 4.5
	7	A	Bolt C.G.	after	1.33	5/16 x 4.5
		B	Bolt C.G.	after	1.33	5/16 x 4.5

3.3.2 Double Shear Fatigue

The testing matrix for the single fatigue test is provided in Table 3.2. The testing matrix consists of 10 combination connections with a 1.5” weld placed about the bolt center of gravity. However, due to time constraints, only the first test was completed at the time of publishing this thesis.

Table 3.2: Double Shear Fatigue Test Matrix

	Test No	Series	Faying Surface Class	Stress Range (ksi)	Weld/Bolt Ratio	Weld Geometry (Size x Length) (in)
Bolted & Welded	F1*	A	A	20	0.67	1/4x 1.5
	F1	B	A	20	0.67	1/4x 1.5
	F2	A	B	20	0.40	1/4x 1.5
	F2	B	B	20	0.40	1/4x 1.5
	F3	A	A	16	0.67	1/4x 1.5
	F3	B	A	16	0.67	1/4x 1.5
	F4	A	B	16	0.40	1/4x 1.5
	F4	B	B	16	0.40	1/4x 1.5
	F5	A	B	12	0.40	1/4x 1.5
	F5	B	B	12	0.40	1/4x 1.5

*Test completed

3.4 EXPERIMENTAL TEST FRAME

3.4.1 Test Frame Characteristics

A test frame in the Bert Cooper Engineering Lab was previously designed and constructed to complete experimental research on quantifying the load-deformation behavior of double shear combination connections. To accomplish the previous testing, this frame was designed to provide over 500 kips of force to the test specimen. This is well above the highest capacity expected in the single shear direct tension testing matrix.

Therefore, this frame was used for all single shear tests without any modifications. Figure 3.3 shows the experimental testing frame and the sample installed before conducting the test.

Figure 3.3: Large-Scale Testing Frame at Bert Cooper Engineering Lab in Stillwater, OK.

The load frame includes an upper header beam connected to a lower beam my two load columns and the test specimen as shown in Figure 3.4 [22]. The upper header beam is fixed in its position to the side support beams of the testing frame. The side support beams are connected using end plate moment connections to the four columns on the outer edges of the test frame. The lower beam rest between two channels which restrain the lateral movement. Each load column is made up of a 565 ton simplex actuator with a 250 kip load cell. Both 565 ton simplex actuators are controlled by a servo valve

connected to an MTS Hydraulic Service Manifold. Additionally, each load column is connected to an MTS Flextest 60 computer to create and execute the load testing procedures.

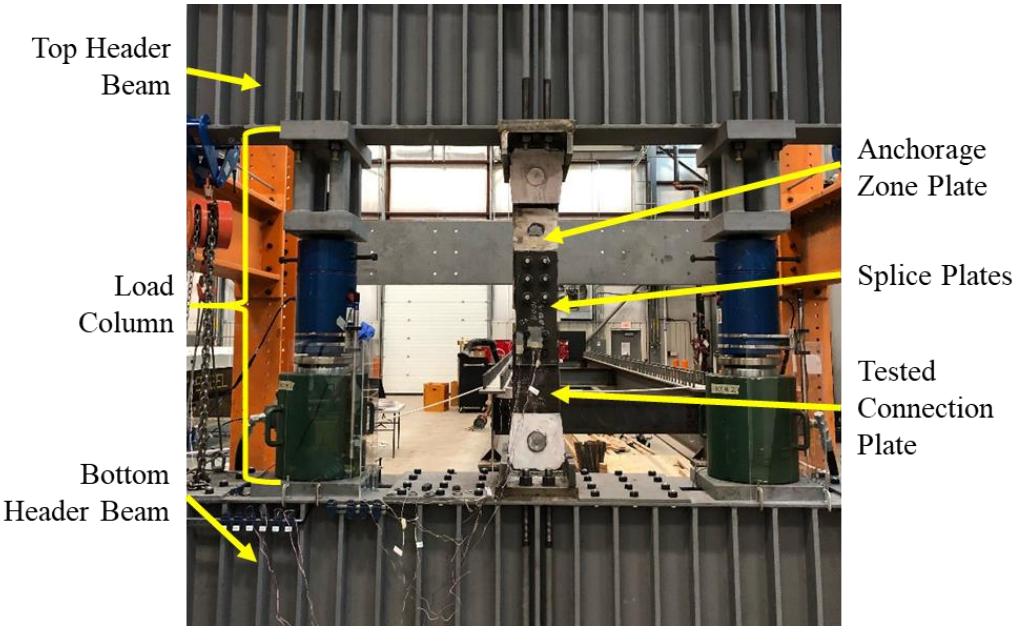

Figure 3.4: Experimental Test Frame for Single Shear Specimen

[Adapted from Understanding the Behavior of Double Shear Axial Lap Steel Connections Made in Combination of Slip-Critical Bolts and Longitudinal Fillet Welds [22]]

3.4.2 Test Frame Modifications for Fatigue Testing

Since the simplex actuators used in the monotonic testing are not fatigue rated, the load frame was modified prior to the start of fatigue testing. This modification included removing each of the existing load columns, made up of a 565 ton simplex actuator and a 250 kip load cell and replacing them with two 55 kip MTS hydraulic actuators. These actuators included integrated displacement and force transducer to allow for load- or displacement-controlled testing. MTS servo valves were also installed on the actuators to

allow for automated control of the tests. While conducting a fatigue tests, the hydraulic actuators will apply a constant amplitude tensile fatigue load that ranges from 5 kips to 110 kips for each cycle. A ramp load is used with rate of 5 inches per minute for the loading and unloading strokes. The test frame with modifications for fatigue testing is shown in Figure 3.5.

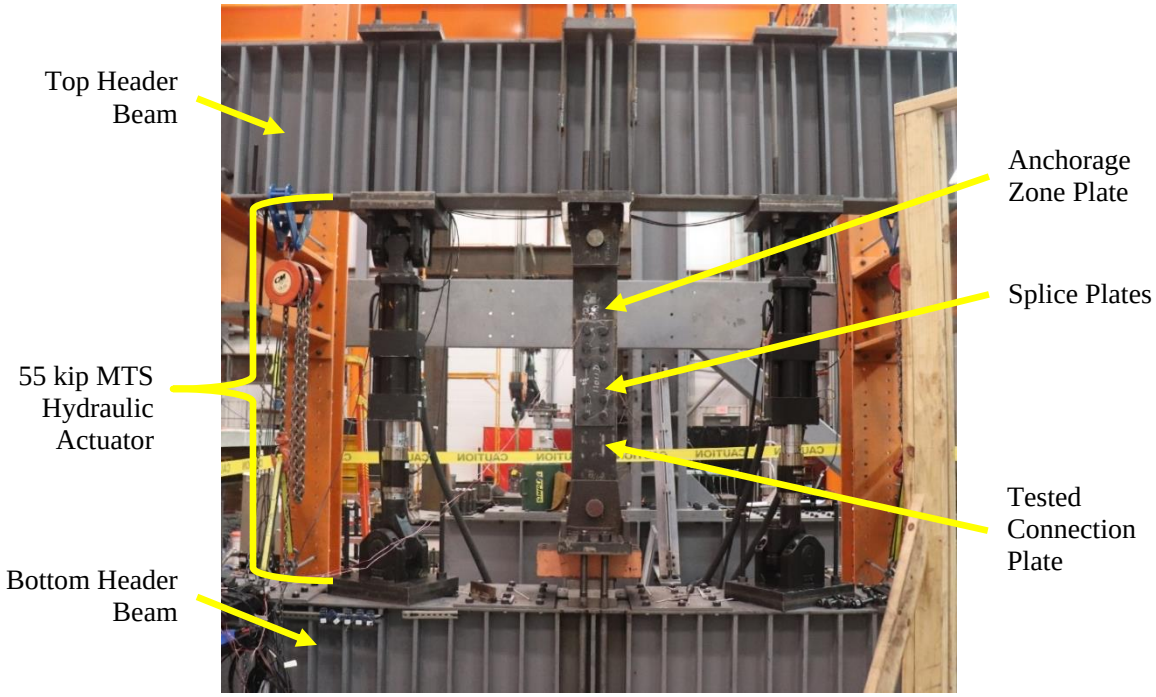

Figure 3.5: Large-Scale Experimental Frame with Fatigue Modifications

3.5 INSTRUMENTATION

3.5.1 Monotonic Testing Instrumentation

For the single shear monotonic tension test, instrumentation was provided to collect the load and displacement (i.e., slip) data using load cells and linear variable displacement

transducers (LVDTs). To record the data during testing, a National Instruments (NI) Data Acquisition system, cDAQ-9178, was chosen for its ability to provide data feedback in real-time through Labview NXG 2.0 software [35].

Four LVDTs (two AC-LVDTs and two DC-LVDTs) were used to measure the slip between the connection plates as load was applied. The slip of the tested connection was captured by two AC-LVDT's installed at the bottom of the splice plate as shown in Figure 3.5. The AC-LVDT's have the ability to obtain displacement data with high resolution and can record up to 0.2 inches of slip. The two DC-LVDTs, shown in Figure 3.6, are used to measure the displacement between the two anchorage zone plates during the test.

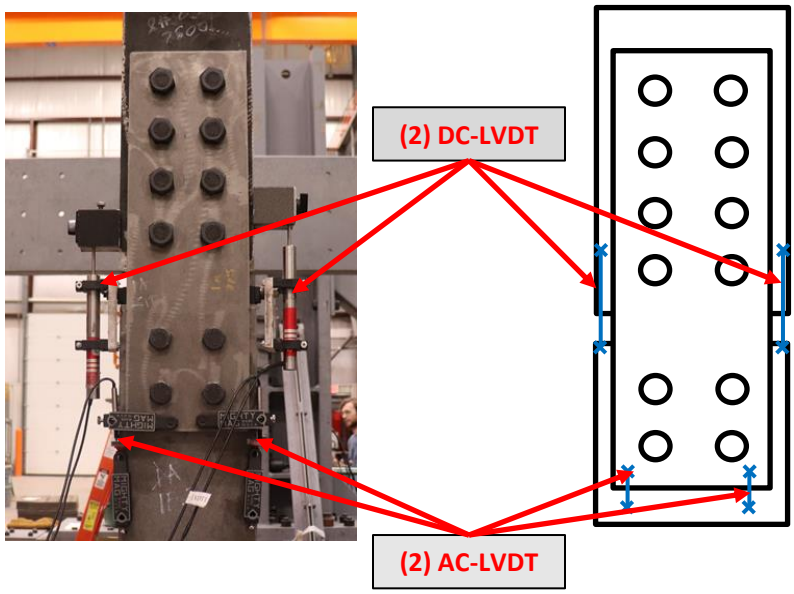

Figure 3.6: Instrumentation on Single Shear Specimen

Force data is captured by the load cells that make up the load column of the testing frame in Figure 3.4. The load cells provide force information to the both the MTS FlexTest 60 controller and the NI cDAQ-9178. The MTS FlexTest 60 controller, with the aid of MTS Multipurpose Elite software, uses the displacement readings of the actuators to run the displacement ramp sequence of the test. The loading rate of the monotonic testing was 0.02 inches per minute. The NI cDAQ-9178 partnered with the Labview NXG 2.0 software is used to generate real-time plots of data as the test is running and also to save the data set to a text file.

3.5.2 Fatigue Instrumentation

In a similar manner as the tension instrumentation, an NI cDAQ-9178 was used to acquire displacement, strain and load data during the fatigue tests. The NI data acquisition system was then paired with an updated Labview NXG 2.0 code to operate with additional instrumentation. The instruments connected to the NI cDAQ-9178 for the fatigue tests included: 4 AC-LVDT's, 2 DC-LVDT's, 8 strain gauges, and 2 analog input signals for load. The fatigue test specimen with all instrumentation is shown in Figure 3.6.

The total slip of the double shear axial lap splice connection used in the fatigue testing was recorded by two AC-LVDT's Additional AC-LVDT’s were placed across the rows of the bolts on the splice plate to measure local compliance.

Additionally, 8 strain gauges were applied to the tested splice plate. The strain gauges can be observed in Figure 3.6. Each strain gauge was purposely placed on the splice plate in

the area adjacent to the toe of the weld. This was done to compare the strain in each location, and quantify changes in strain during crack propagation.

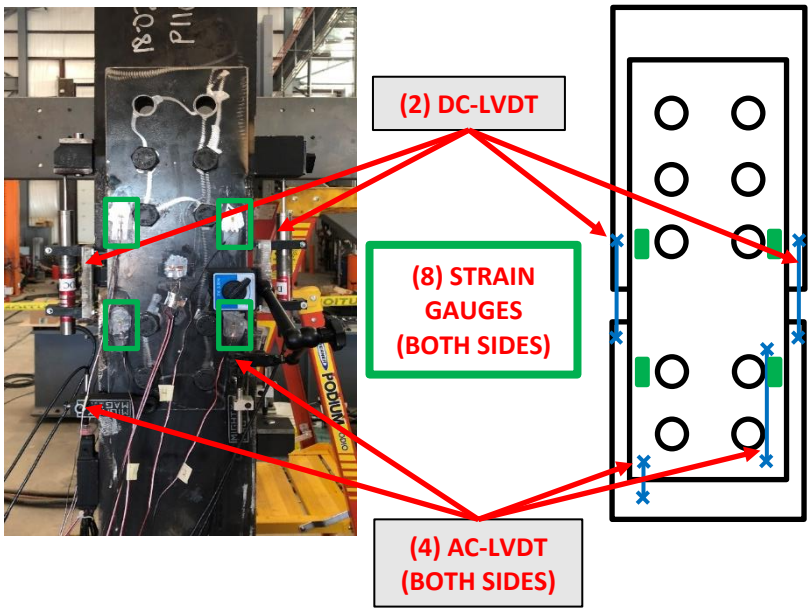

Figure 3.7: Instrumentation on Fatigue Specimen

The load cells used in monotonic tension testing were replaced with two 55 kip MTS actuators. Since only one port was available on the load cell of the MTS actuator, the signal was first sent to the MTS Flextest 60 controller. A voltage output was created on the MTS Flextest 60 controller to send the load signal to the NI cDAQ-9178. Once the data acquisition system was configured correctly, the load reading was calibrated within the Labview NXG 2.0 code to match the load reading on the MTS controller.

3.6 TEST PROCEDURE

3.6.1 Tension Procedure

A systematic procedure was created to ensure consistency with testing operation. The procedure used to complete tension testing is as follows.

1. Clean the faying surface of the Class B connections using high pressure air. This ensures all the dust and other particles are removed.
2. Lift the upper and lower grip plates into respective positions and insert the 3-in pin through the grip plate and grip connection.
3. Attach the splice plate to a single side of the grip plates and snug tighten the upper bolts. The upper bolts are 7/8-in A490 bolts that will be in bearing with the grip and splice plate.
4. Place the tested connection bolts in negative bearing. To do so, raise the lower beam of the test frame by using the hydraulic actuators. When the holes of the tested connection region are aligned in the negative bearing orientation, the bolts may be installed.
5. Test three A325 ¾-in bolts in the Skidmore Wilhelm bolt tension calibrator and record values on a testing sheet.
6. Assemble the test bolts in the tested connection region and pretension each bolt using the turn of nut (ToN) method. See RCSC Specification (Table J3.1 AISC) [28].
7. Install welds on the tested connection according to the respective weld size in the testing matrix. Record all As-Built dimensions of the weld.
8. Attach all testing instrumentation. This includes all LVDT's and webcams.

9. Open the MTS Multipurpose Test Suite Application and open the test template for monotonic tension testing. This software is used to control the MTS FlexTest 60 controller. Each tension test is performed by displacing the hydraulic actuators at a rate of 0.02 in/min.
10. After complete fracture of the welds, bearing of the test bolts, or a slip of 0.2-in is reached, the test is stopped. The tested connection is removed entirely, and the weld fracture areas are measured.

3.6.2 Fatigue Testing Procedure

The following procedure were created for testing the combination connections under fatigue loading:

1. Clean the faying surface of the Class A connections by spraying with pressurized air. This removes dust and other particles that can reduce the slip resistance of the connection.
2. Assemble the connection grips to the testing frame. Start by lifting the upper grip and lower grip into their respective positions and attaching to the frame by inserting the 3-in pin through the grip plate and grip plate connection.
3. Assemble the splice plates to the grip plates. The fatigue test is being conducted on a double shear connection, therefore a splice plate should be installed on both sides of the test grip plate. All bolts are installed so that no bearing occurs between the bolt shanks by either the grip or splice plate. Once all bolts are centered in their holes, the bolts are snug tightened.

4. Perform three tests on A325 ¾-in bolts using the Skidmore Wilhelm bolt tension calibrator and record values on a testing sheet.
5. Pretension each bolt using the turn of nut (ToN) method. See RCSC Specification (Table J3.1 AISC).
6. Install welds on the tested connection according to the respective weld size in the testing matrix. Record all As-Built dimensions of the weld.
7. Attach all testing instrumentation.
    a. 4 AC-LVDT's
    b. 2 DC-LVDT's
    c. 8 Strain Gauges
    d. Webcams
8. Open the MTS Multipurpose Test Suite Application and run the test template for fatigue testing.
9. After a complete loss in stiffness (i.e., fracture in one of the plates), the fatigue test operation is stopped. The test specimen is removed, the total number of cycles is recorded and the specimen is examined in further detail.

CHAPTER IV

4 EXPERIMENTAL RESULTS

4.1 INTRODUCTION

A total of 12 connections were tested under the single shear portion of this experimental testing program. Each specimen was tested until fracture of the weld occurs, a slip of 0.2-in is reached or bearing of the bolts was observed. In all tests inclusive of a weld, welded-only and combination specimens, the tests were stopped when weld fracture occurred. As a result of eccentricity in the connection, secondary bending effects were observed during the single shear testing. This produced a combined bending and axial stress effect in the test specimen.

As indicated above, fatigue specimens consisted of a class A faying surface with a 2x2 bolt pattern and 1.5-in fillet welds placed about the bolt center of gravity. The failure of a fatigue specimen was met when a significant loss of stiffness occurred.

In section 4.2 of this chapter, the AISC prediction for the single shear joint is described. Section 4.3 discusses the As-Built prediction for the single shear joint. Section 4.4 highlights the criteria used to determine the slip capacity of the single shear test specimens based on its load-deformation (i.e., load-slip) behavior. Section 4.5 is

is organized into 3 sub-sections to present the testing results of various configurations: Bolted Only, Welded Only and Combination Connections. The load-deformation response of each test specimen is examined. Section 4.6 explains the failure criteria defined in the fatigue testing of double shear connections while Section 4.7 presents the data collected throughout the experimental fatigue testing program.

4.2 AISC Single Shear Connection Capacity

The nominal strength for single shear joints as defined by AISC is a function of the number of slip planes, and therefore, the single shear joint is predicted as one-half the capacity of the double shear joint. For bolts and welds in a shared load system AISC recommends the direct addition of bolt R_n and weld R_n. Defined as R_{nb} and R_{nw} below.

AISC Slip Critical Bolts:

$$R_{nb} = \mu D_u h_f T_b n_s \qquad \text{Eq. 16 (AISC J3-4) [2]}$$

h_f = 1.0; Factor for fillers

D_u = 1.13; a multiplier that reflects the ratio of the mean installed bolt pretension to the specified minimum pretension

T_b = Minimum fastener pretension considered as 28 kips for 3/4-in A325 bolts

n_s = 1; Number of slip planes required to permit the connection to slip

μ= Mean slip coefficient for Class A or B surfaces. μ = 0.3 for Class A and μ = 0.5 for Class B

AISC Fillet Welds:

$$R_{nw} = 0.6F_{EXX}\left(\frac{\sqrt{2}}{2}\right)\left(\frac{D}{16}\right)l \qquad \text{Eq. 87 (AISC 8-1) [7]}$$

$F_{EXX} = 70\ ksi;\ Filler\ metal\ clasification\ strength$ = 70 ksi; Filler metal classification strength

$D = 5;\ weld\ size\ in\ sixteenths\ of\ an\ inch$ = 5; Weld size in sixteenths of an inch

l = Length of weld, in

The weld to bolt strength ratio is computed as

$$Ratio = \frac{R_{nw}}{R_{nb}} \qquad \text{Eq. 18}$$

4.3 As-Built Single Shear Connection Capacity

To judge the accuracy of the AISC in predicting the capacity of the tested connections, the actual properties of fasteners identified during the testing program is used in conjunction with the AISC nominal capacity formulation. The resulting capacity is denoted the As-Built capacity. A similar prediction was performed in Soliman, et al [11] based on the results of testing 75 double shear combination connections. This prediction utilizes the actual dimensions of the weld after installation, the average bolt pretension supplied by the bolts (measured using the Skidmore), and the weld ultimate shear strength obtained from the welded-only tests. Below is a summary of how to compute the As-Built capacity for a single shear connection with a Class B faying surface.

As-Built Capacity of Slip-Critical Bolts:

$$R_b = \mu h_f n_s T_B \qquad \text{Eq. 19 [11]}$$

$\mu =$ Experimental slip coefficient for Class A or B surfaces. μ = 0.535 for Class B

h_f = 1.0; Factor for fillers (no fillers)

n_s= 1; Number of slip planes required to permit the connection to slip

T_B= Fastener pretension: $T_b = 42.73\ kips$ for 3/4-in. A325 – ToN [22]

As-Built Capacity of Fillet Welds:

$$R_w = \tau t_e l \qquad \text{Eq. 20 [11]}$$

τ= 69.29 ksi; Weld ultimate shear stress [11]

$t_e = \frac{ab}{\sqrt{a^2+b^2}}$; The shortest distance of the weld from the root to the face of the weld, where a and b are the measured legs of the fillet weld. This accommodates unequal leg sizes. (Salmon et al. 2009)

l= Weld length, in.

Then the As-Built capacity of the combination connection is

$$R_n = R_b + R_w \qquad \text{Eq.21 [11]}$$

4.4 Determination of the Single Shear Experimental Slip and Ultimate Capacities

The Research Council on Structural Steel Connections (RCSC) [28] provides guidance on identifying, experimentally, the friction coefficient of slip-critical joints. Three respective load-deformation responses of slip critical connections have been outlined by the RCSC. These criteria defined for estimating the friction coefficient are used to establish the slip capacity of the tested connections. The three different load-deformation profiles can be observed in Figure 4.1. Based on these profiles, the slip capacity of the three profiles given in Figure 4.1 is as follows:

- For Profile (a), the slip load is determined as the maximum load that occurs prior to a slip of 0.02-in.

- For Profile (b), the slip load is determined at the point at which the slip rate increases suddenly.
- For Profile (c), the slip load is the load corresponding to a deformation of 0.02”

For the Class B bolted-only specimens, the load-deformation curve followed a response similar to Case (a), reaching its peak prior to 0.02” of slip. This was also observed for double shear combination connections tested in Soliman et al. [11]. However, due to the secondary bending stresses, single shear combination joint followed a behavior similar to that of Case (c). Furthermore, whereas the slip capacity of double shear combination connections tested in [11] could reach more than 90% of the ultimate capacity of the connection, the single shear combination connections would display an ultimate force that can be significantly higher that the slip load identified above. As a result, two capacities have been provided and analyzed in this thesis based on the load-deformation behavior of the single shear connections. The first is the slip capacity of the connection and the second is the ultimate capacity (i.e., maximum force carried by the connection before weld failure or bolts reaching bearing state). This capacity was analyzed since the load-deformation curve of the single shear combination joint displays a gradual increase in capacity beyond the defined 0.02” point of predicting slip capacity outlined by the RCSC.

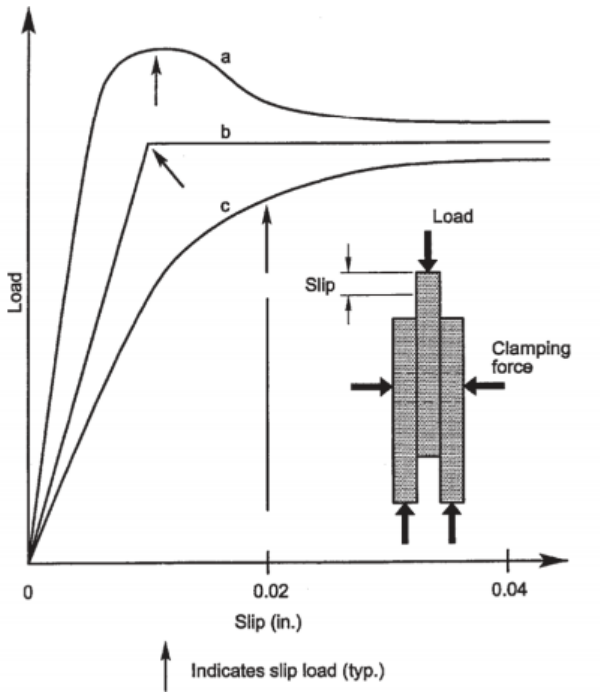

Figure 4.1: Evaluation of Slip Capacity

[Adapted from *Specification for Structural Joints Using High-Strength Bolts [28]*]

4.5 Single Shear Testing Results

4.5.1 Bolted-Only

A single bolted-only test was performed prior to the testing of the combination joint to observe the behavior of the individual fastener. The test was constructed of a 2x2 bolt configuration with A325 ¾-in bolts and a Class B faying surface. Each bolt was pretensioned by using the ToN method. Table 4.1 shows the characteristics of the bolted-only test within the full testing matrix.

Table 4.1: Bolted-Only Testing Matrix

	Test No	Series	Weld Location	Assembly Sequence (Pretension before/after Weld)	Weld/Bolt Ratio	Weld Geometry (Size x Length) (in)
Bolted-Only	1	A	Bolt C.G.	before	---	---

Figure 4.2 shows the load-deformation response for the single bolted-only test. The load-deformation response of the bolted-only joint displayed slip behavior relative to that of Case (a) outlined by RCSC [28]. Therefore, the slip capacity of the bolted-only connection was determined to be 65.61 kips. It should be noted that the AISC nominal capacity for this connection is 63.30 kips which is 3.6% lower than the experimental outcome.

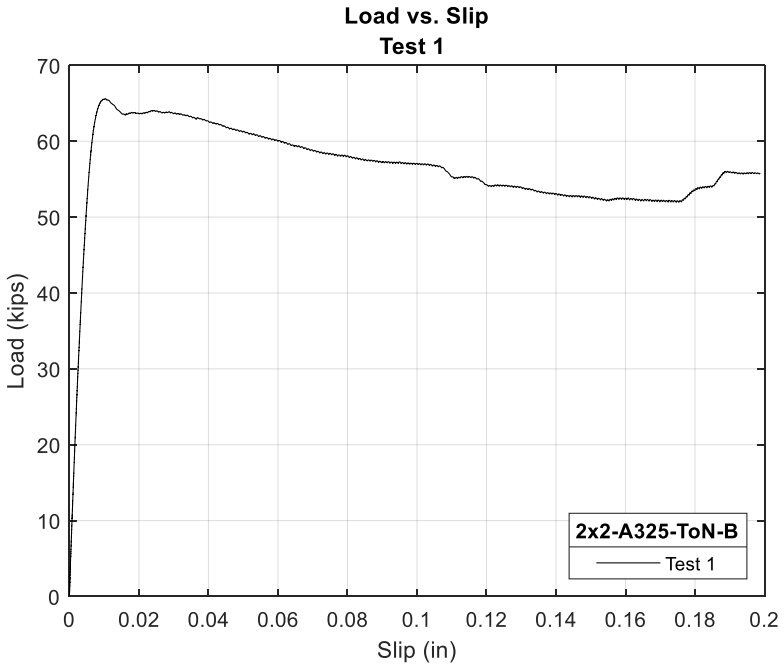

Figure 4.2: Bolted-Only Load-Deformation Response

4.5.2 Welded-Only

A test was performed on a single welded-only connection prior to testing of the combination connection to characterize the behavior of the individual fastener element. The welded-only test consisted of a Class B splice plate with 4.5-in weld as outlined in Table 4.2, the welded-only portion of the testing matrix.

Table 4.2: Welded-Only Testing Matrix

	Test No	Series	Weld Location	Assembly Sequence (Pretension before/after Weld)	Weld/Bolt Ratio	Weld Geometry (Size x Length) (in)
Welded-Only	2	A	Bolt C.G.	before	---	5/16 x 4.5

The load-deformation relationship of the single shear welded-only test is provided in Figure 4.3. The load-deformation response of the welded-only joint displayed a higher initial stiffness (recorded at a slip of 0.005") compared to the bolted-only case (i.e., 10,340 kip/in for the bolted-only compared to 11,735 kip/inch for the welded only). The ultimate capacity was 124.72 kips at a slip of 0.04-in. After reaching the ultimate load, the load carried by the welded-only connection gradually decreased. This is due to the developing fracture of the welds in the test specimen as slip increased.

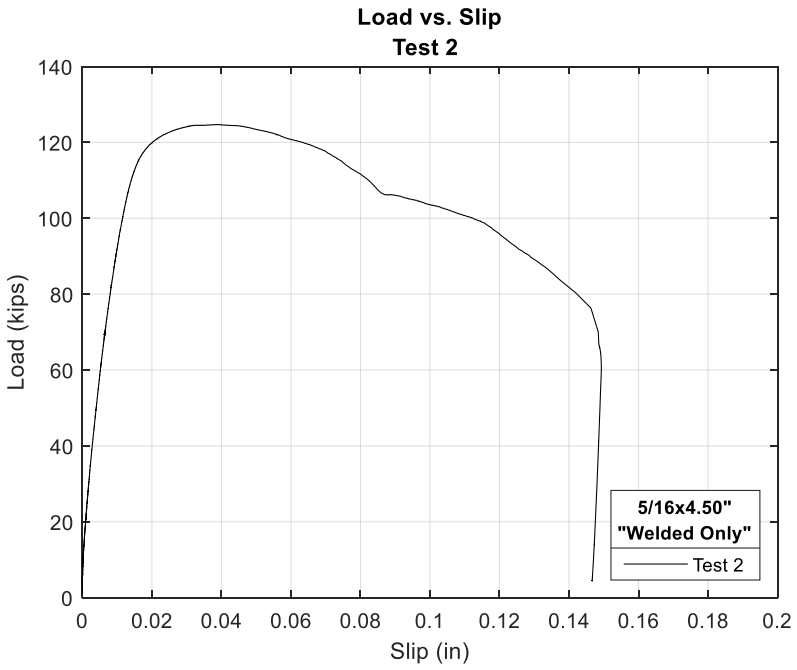

Figure 4.3: Welded-Only Load-Deformation Response

4.5.3 Combination Connections

The experimental testing performed on combination connections includes Test 3,4,5,6, and 7. Each test was completed on two specimens represented by “A” or “B” after the test number. The combination section of the testing matrix is presented in Table 4.3.

Table 4.3: Combination Connection Testing Matrix

	Test No	Series	Weld Location	Assembly Sequence (Pretension before/after Weld)	Weld/Bolt Ratio	Weld Geometry (Size x Length) (in)
Bolted & Welded	3	A	Bolt C.G.	before	0.9	5/16 x 3
		B	Bolt C.G.	before	0.9	5/16 x 3
	4	A	Bolt C.G.	before	1.33	5/16 x 4.5
		B	Bolt C.G.	before	1.33	5/16 x 4.5
	5	A	Above Bolt C.G.	before	1.33	5/16 x 4.5
		B	Above Bolt C.G.	before	1.33	5/16 x 4.5
	6	A	Below Bolt C.G.	before	1.33	5/16 x 4.5
		B	Below Bolt C.G.	before	1.33	5/16 x 4.5
	7	A	Bolt C.G.	after	1.33	5/16 x 4.5
		B	Bolt C.G.	after	1.33	5/16 x 4.5

All tested specimens were 7/8-in thick plates with a Class B faying surface constructed of slip-critical A325 3/4-in bolts and longitudinal fillet welds.

The load-deformation profiles of Test 3 are shown in Figure 4.4. In this test, a longitudinal weld length of 3-in was placed at the bolt center of gravity on both sides of the single shear splice plate. Both Test 3A and 3B displayed a consistent initial stiffness as displayed in Figure 4.4. The initial stiffness is higher than that of the bolted-only and welded-only cases (an average of 12,034 kip/in for Test 3). At a slip of 0.02-in, Test 3A and Test 3B were at a load of 152.51 kips and 147.64 kips, respectively. This would be their slip capacity according to the criteria defined above. The ultimate load sustained in Test 3A and Test 3B was 170.96 kips and 167.71 kips, respectively. A failure was observed in Test 3A and 3B when the welds fractured. The nominal AISC capacity for this configuration was calculated as 119.00 kips.

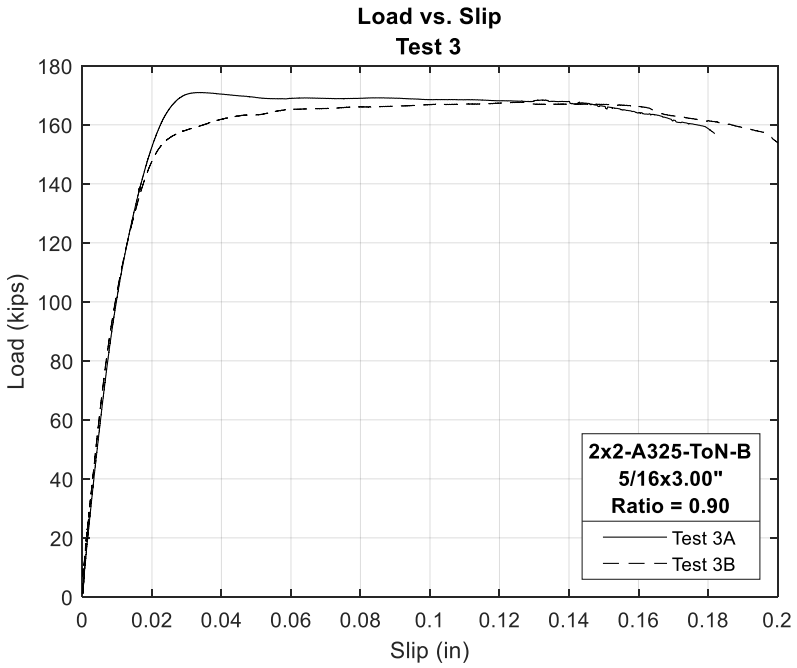

Figure 4.4: Test 3 load-deformation response

Test 4 was the first test of the combination joints that contained a 4.5-in weld. A resulting weld to bolt ratio for this configuration was calculated to be 1.33 as shown in Table 4.3. The mean initial stiffness of Test 4A and Test 4B appears to be very similar to that of Test 3A and Test 3B (5% difference in initial stiffness). Once the slip of the connection reached the value of 0.02-in, the slip capacity was found to be 165.45 kips and 178.43 kips, representing a significantly lower value than the ultimate capacity of 222.04 kips and 224.86 kips for both tests, respectively. For Test 4,5,6 and 7 the AISC capacity was calculated to be 146.80 kips and the failure was determined as the fracturing of welds.

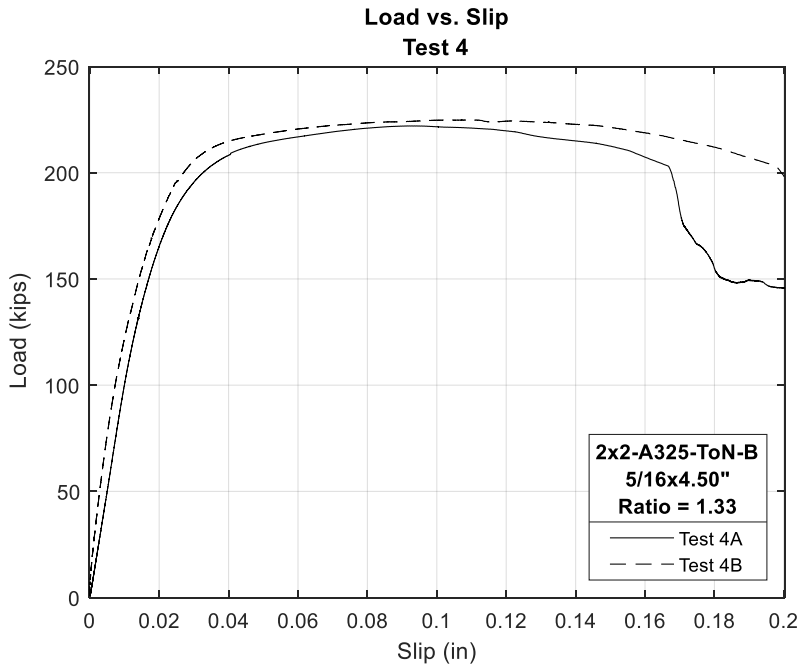

Figure 4.5: Test 4 Load-Deformation Response

Test 5 was the second series of tests completed with a 4.5-in longitudinal fillet weld. Test 5 and 6 were designed to assess the effect of changing the weld location with respect to center of gravity of bolts on the load-deformation behavior of the connection. Since connections in Test 4 displayed significant bending during the tests due to the secondary bending effects, the stresses on the weld lines were not uniformly distributed and the stress fields within the welds can change with the weld location. The weld location in Tests 4,5, and 6 is shown in Figure 4.6 below.

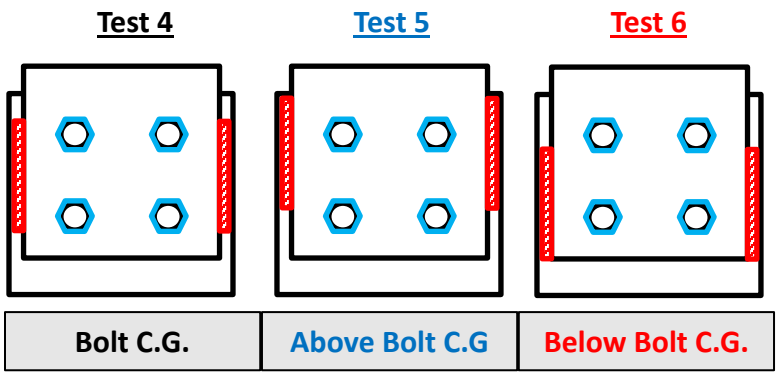

Figure 4.6: Schematic of Weld Location

For Test 5, the welds were placed above the center of gravity of bolts. The load-deformation curves are provided in Figure 4.7. At a slip of 0.02-in, the load carried by the connection in Test 5A was 169.67 kips and Test 5B was 171.59 kips, similar to the mean slip capacity of Test 4. However, the ultimate load of Test 5A and Test 5B was determined to be 212.26 kips and 232.45 kip, respectively. Test 6 also consisted of a 4.5-in longitudinal fillet welds similar to that of Test 4 and Test 5. However, the welds for this series of testing were placed below the bolt center of gravity. The load-deformation response is shown in Figure 4.9. When the respective test reached a slip of 0.02-in, the load within the connection was determined to be 204.76 kips for Test 6A and 204.46 kips for Test 6B. Additionally, the ultimate capacity of Test 6A was determined to be 221.06 kips and Test 6B to be 246.77 kips. These results will be analyzed in Chapter 5 to discuss the effect of the weld location on the capacity of the connection.

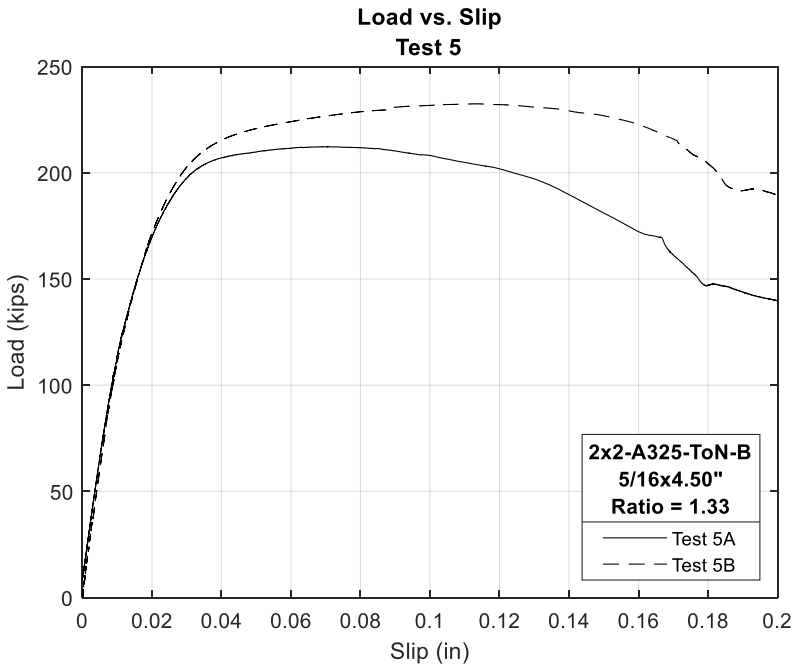

Figure 4.7: Test 5 Load-Deformation Response

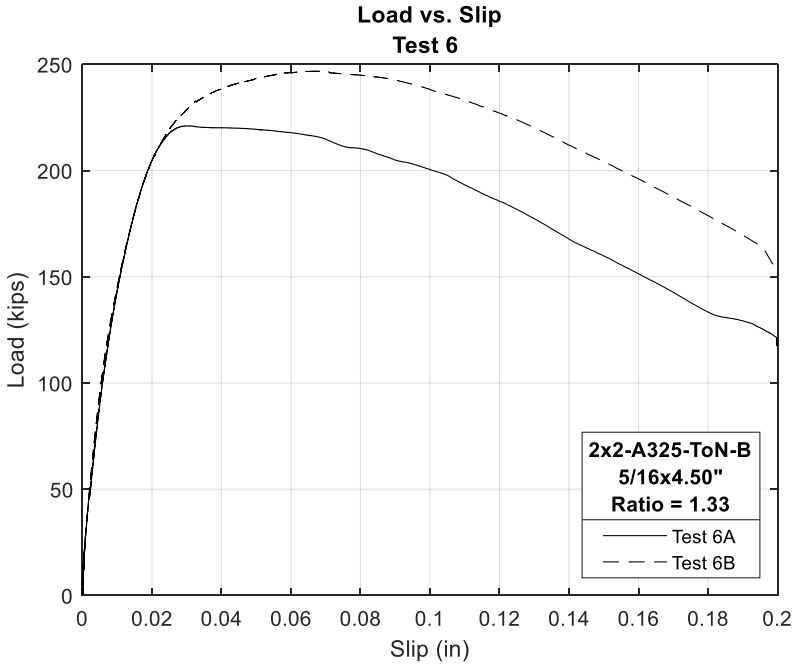

Figure 4.8: Test 6 Load-Deformation Response

Test 7 once again utilized the 4.5-in longitudinal fillet weld in combination with pretensioned bolts. In Test 7 the welds were placed about the bolts center of gravity. However, for this series, the welds were installed before any applied pretension force to the bolt group. The load-deformation response is illustrated in Figure 4.9. At a slip of 0.02-in the force was reported as 140.00 kips for Test 7A and 185.47 kips for Test 7B. The ultimate capacity of Test 7A and 7B was determined to be 195.93 kips and 232.68 kips, respectively.

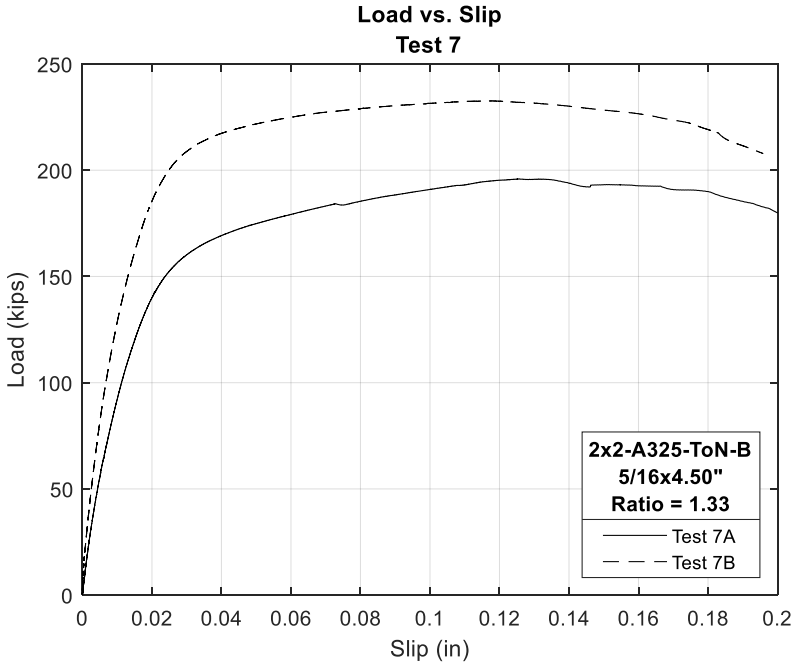

Figure 4.9: Test 7 Load-Deformation Response

4.6 Fatigue Testing Considerations

Several considerations were made to determine the failure criteria of the fatigue test specimens. One such consideration was to conclude the fatigue test after a crack had initiated at the plate edge and propagated to the closest bolt holt similar to the failure

criteria used in the study by Bowman [20]. However, it was found that once this stage of testing was reached, the connection could still provide sufficient stiffness and strength to carry the fatigue load. Therefore, high cycle loading was continued until the connection had shown a complete loss in stiffness. This case corresponded to a complete fracture of one of the two splice plates. To assess the behavior of the connection as the cracks propagated, the stiffness of the specimen was calculated.

The stiffness was calculated based on the referenced global system shown in Figure 4.10. This stiffness relies on the load and displacement data acquired within the 55 kip MTS Duraglide actuator. The stiffness is computed as the slope of the load-deformation for each respective cycle in the fatigue test.

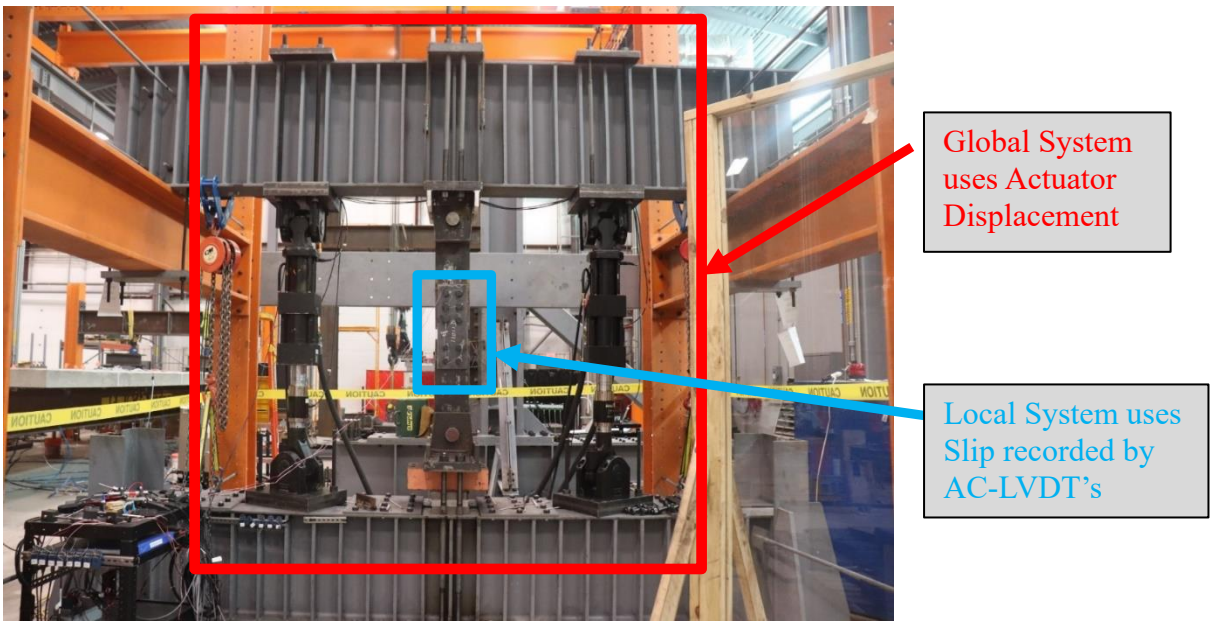

Figure 4.10: Global and Local System referred to in Fatigue Testing

4.7 Fatigue Testing Results

4.7.1 Behavior of Test Specimen

Due to the time required to conduct the fatigue tests, as of writing this thesis, one test was completed, and a second test was in the final phases of completion. However, this thesis only reports the results on the first test. These tests were performed on a double shear lap splice connection with bolts and welds in combination. The completed test is denoted Test F1 herein. The test procedure consisted of constant amplitude loading with a peak of 110 kips and a valley of 5 kips in tension. The two splice plates used in the testing had a combined nominal area of 5.25 in^2, resulting in a total change in stress of approximately 20 ksi based on the gross area of the connection. It is typical to use the gross cross-sectional area of plates when pretensioned bolts are utilized [18]. Accordingly, the gross cross-sectional area was used to compute the stress range for the case of bolts and welds in a shared load system. Table 4.4 shows the cracking stages with respect to the number of cycles. No immediate increase in slip deformation was observed with crack initiation. The connection was able to maintain its resistance to the load while cracks propagated and gradual slip between the plates ensued. After initial cracking occurred, the combination connection possessed a reserve capacity which extended the total fatigue life of the connection.

Test F1 was conducted until the total number of cycles reached 1,399,748. At that point the connection had such a loss in stiffness that it could not carry the peak of the cyclic load, and both splice plates fractured before the test was stopped. Observing the test data, a change in the initial stiffness was not significant until failure occurred. However, the

connection displayed an increase in slip deformation as the number of cycles increased. Figure 4.10 shows the load-slip displacement of the specimen at 14,786 cycles and 1,346,603 cycles.

Table 4.4: Occurrences of cracking observed in Test F1

Behavior	Cycles
Crack #1 Initiation @ SG3	436,799
Crack #2 Initiation @ SG7	699,773
Crack #3 Initiation @ SG8	724,773
Crack#2 (SG3) Reaches Hole & Crack #4 Ititiation @SG6	774,773
Crack #5 Initiation @ SG2	954,760
Crack #6 Initiation @ SG4	1,130,315
Crack Propogation between Bolt Holes	1,346,603
Loss of Stiffness	1,399,748

Category	Cycles
E	137,500
D	275,000
C	550,000
B	1,500,000

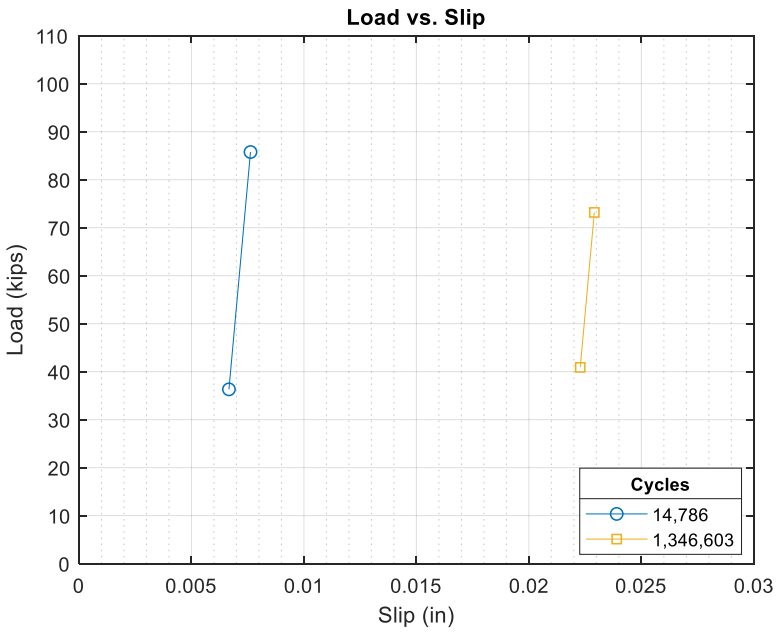

Figure 4.11: Slip of Fatigue Test Specimen with respect to number of cycles

CHAPTER V

5 DISCUSSION

5.1 INTRODUCTION

This experimental testing program was constructed to provide more insight on the behavior of axial lap steel connections with bolts and welds in a single shared load system. This chapter discusses the results of both the single shear monotonic and the double shear fatigue testing. The discussion of single shear results includes: an investigation into the effects of weld location, quantifying the effect of connecting element placement sequence, a comparison between the single shear results and double shear results obtained from previous testing here at Oklahoma State University [11,22], numerical analysis of the test results by finite element modeling, a parametric study on plate thickness and weld length, and finally a comparison of experimental results with the AISC prediction model as well as the As-Built prediction model. The summary of fatigue testing includes an investigation of the crack propagation throughout the test and a comparison to the AASHTO fatigue detail categories.

Section 5.2 evaluates the results of all single shear monotonic tension tests while Section 5.3 evaluates the results of the double shear fatigue test.

5.2 SINGLE SHEAR TENSION MONOTONIC TESTING

5.2.1 Effect of Weld Location

The impact of weld location with respect to the center of gravity of bolts in the combination connection was studied using the results of Test 4 – Test 6. Each test had its respective weld location about the bolt center of gravity: Test 4 – About the bolt center, Test 5 – Above the bolt center, and Test 6 – Below the bolt center. Figure 5.1 (a), (b) and (c) illustrate the weld placement with respect to the bolt center of gravity.

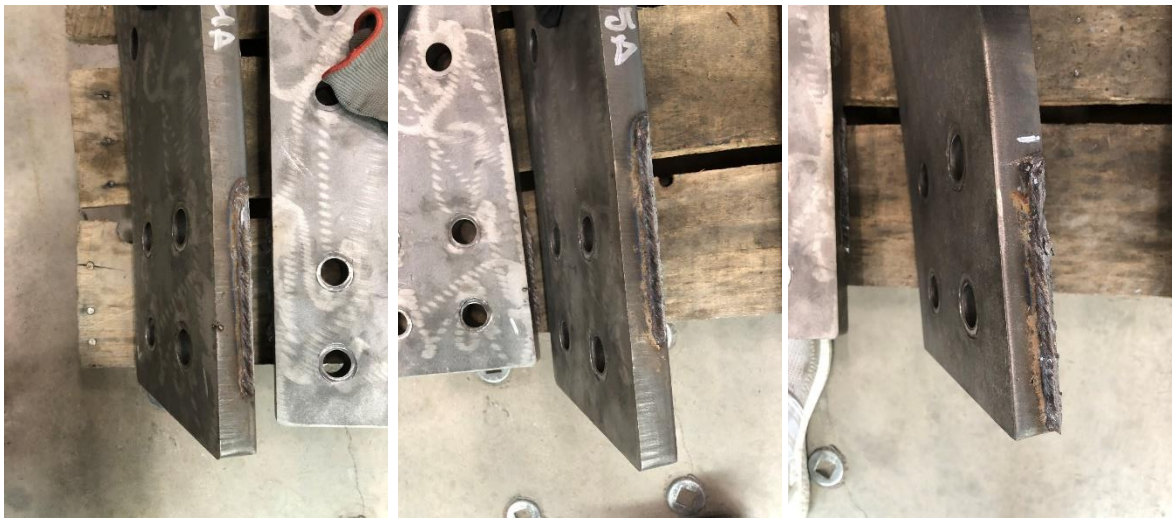

(a) (b) (c)

Figure 5.1: Location of weld on Test Specimen (a) About bolt Center of Gravity (Test 4) (b) Above bolt Center of Gravity (Test 5) (c) Below Bolt Center of Gravity (Test 6)

The load-deformation behavior of the three test configurations is presented in Figure 5.2. From the figure, it can be observed that Test 4 and Test 5 performed very similar to one another until the slip distance of 0.04-in. However, Test 6 displayed a different behavior throughout the test compared to Tests 4 and 5. As seen in Figure 5.2, the average initial stiffness of Test 6 is 46.9% (12,624.5 kips/in for Test 4, 12,618.9 kips/in for Test 5, and 18536.8 kips/in for Test 6)higher than Tests 4 or 5. Likewise, the slip capacity (i.e., force in the connection at 0.02-in of slip) of Test 6 is on average 19.5% higher than achieved in

Tests 4 and 5. In Table 5.1 the average slip capacity of Test 6 is compared with the average slip capacity of Test 4 and Test 5. This increase in the slip capacity can be attributed to the differences observed in the weld fracture plane. After investigation of the welds post-fracture, the welds included in Test 6 presented a larger surface area along the weld fracture compared to Test 4 and 5. Therefore, it is reasonable to conclude a weld placed below the center of gravity of the pretensioned bolts can behave with greater strength and reduced ductility, similar to the behavior that has been observed in transverse welds [3].

Additionally, based on the data reported in the figure, it can be seen that the variability in the results of Tests 5 and 6 is higher than that in Test 4. This can be attributed to the weld placement further away from the bolt center of gravity.

Table 5.1: Comparison of Test Slip Capacity with different weld locations

	Test No	**Test Slip Capacity (kips)**	**Average**	**SD**	**COV**
Bolted & Welded	4	165.45	171.942	9.181	5.340%
		178.434			
	5	169.672	170.629	1.353	0.793%
		171.585			
	6	204.76	204.610	0.212	0.104%
		204.46			

Table 5.2: Comparison of Test Ultimate Capacity with different weld locations

	Test No	Test Ult. Capacity (kips)	Average	SD	COV
Bolted & Welded	4	222.04	223.450	1.994	0.892%
		224.86			
	5	212.26	222.355	14.276	6.421%
		232.45			
	6	221.06	233.915	18.180	7.772%
		246.77			

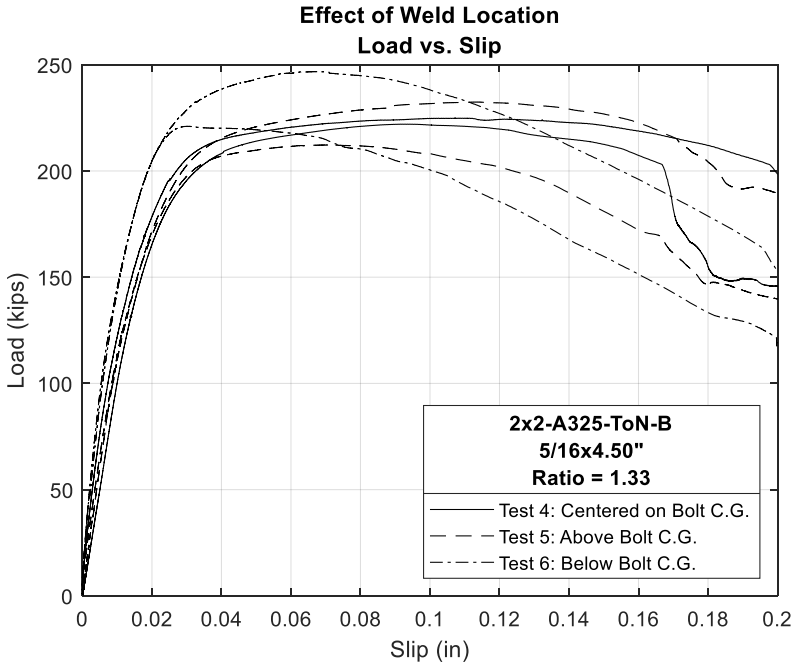

Figure 5.2: Effect of Weld Location

5.2.2 Effect of Connection Assembly Sequence

In Test 4 and Test 7, the assembly process was altered to determine the effects of connection assembly sequence. In all connections tested in [11], bolts were fully pretensioned before placing the welds. This assembly sequence was chosen to ensure that

the gaps between connection plates are closed to enable developing the full slip resistance of the joint. The Eurocode 3: Design of steel structures - Part 1-8: Design of joints (EN 1993-1-8:2005) [36] allows the use of combination connections, denoted Hybrid connections in [36], made with slip-critical bolts and welds. In [36], the slip-critical bolts can be assumed to share the load with welds provided that the final tightening of the bolts is carried out after the welding is complete. Accordingly, it was of interest to the research team to quantify whether the assembly sequence can affect the behavior of these combination connections.

To accomplish this task, in Test 7 welding was completed before bolt pretensioning was established. The mechanical characteristics of the tested specimens remained the same: A325 bolts tensioned using the ToN method, 4.5-in longitudinal fillet welds, and Class B splice plates. The comparison of Test 4 and Test 7 load-deformation behavior is illustrated in Figure 5.3.

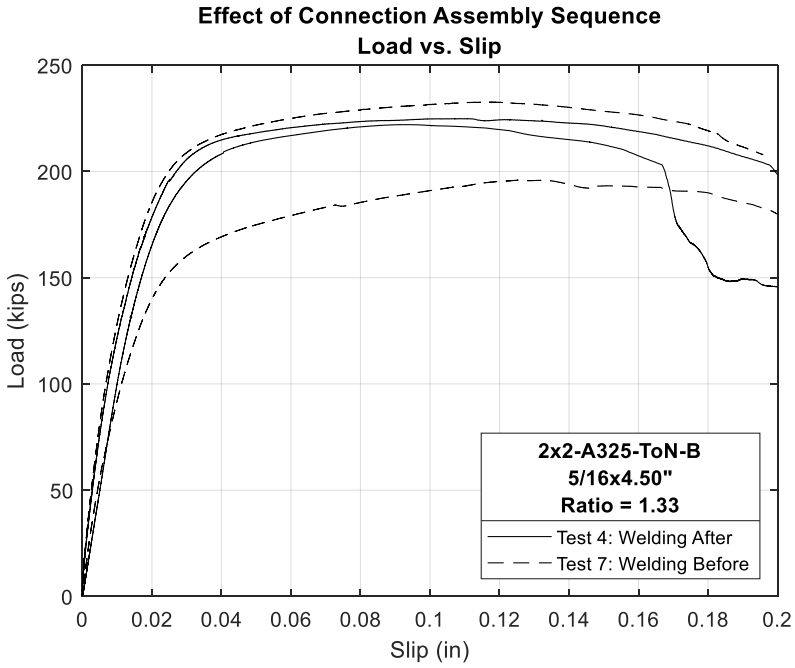

Figure 5.3: Effect of Connection Assembly Sequence

Following the expectations of the research team, Test 7 displays a greater variability in its load-deformation response in comparison to the results of Test 4. The variance of the slip and ultimate capacity of Test 4 and Test 7 is displayed in Table 5.3 and Table 5.4. In both the cases of Test Slip Capacity and Test Ultimate Capacity, the results of Test 7 displayed a high variance in comparison to the results of Test 4. This behavior may be attributed to the presence of small gaps between the slip surfaces, prior to pretensioning the bolts, that may prevent developing the full slip capacity of the bolts. These gaps may be present before welding or can form during welding due to differential heating and cooling of the welded plates.

Table 5.3: Comparison of Slip Capacity with different assembly sequences

	Test No	Test Slip Capacity (kips)	Average	SD	COV
Bolted & Welded	4	165.45	171.942	9.181	5.340%
		178.43			
	7	140.00	162.734	32.151	19.757%
		185.47			

Table 5.4: Comparison of Ultimate Capacity with different assembly sequences

	Test No	Test Ult. Capacity (kips)	Average	SD	COV
Bolted & Welded	4	222.04	223.450	1.994	0.892%
		224.86			
	7	195.93	214.305	25.986	12.126%
		232.68			

As discussed by Heistermann [14], if plates of a bolted connection are assembled with gaps between them, the slip capacity of the connection can be reduced [14]. Heistermann [14] indicated this reduction can reach up to 10.7%. A similar reduction was observed in Test 7A of this study. Although the plates were clamped together and welded in a lab setting, it still was not possible to achieve consistent results when welds are placed prior to the pretensioning of bolts.

5.2.3 Effect of Secondary Bending on the Combination Connection Behavior

Single shear axial lap connections induce loading eccentricity that cannot be practically avoided. As discussed above, this loading eccentricity leads to secondary bending effects that may alter the behavior of the connection. To assess the effect of this bending, a

comparison was performed between Test 3 and Test 4 of this experimental study and *Test 7* and *Test 9* of a previous study conducted on double shear connections [11,22]. Both configurations consisted of a 2x2 bolt layout, A325 bolts tensioned using the ToN method, and Class B faying surfaces. Test 4 and Test 3 in this experimental program is a single shear axial-lap combination connection with a weld size of 5/16x4.5-in and 5/16x3.0-in, respectively. Likewise, *Test 7* and *Test 9* were conducted in the previous study on double shear axial-lap combination connections with a weld size of 5/16x5.0-in and 5/16x3.5-in, respectively [11,22]. Although the nominal weld sizes in the double shear connection are 0.5-in larger than those specified in the single shear connections, comparison of the results can still provide a deeper insight into the effect of secondary bending.

Figure 5.4 displays the load-deformation response of Test 4 (single shear) and *Test 7* (double shear [11,22]) while Figure 5.5 displays the load-deformation response of Test 3 (single shear) and *Test 9* (double shear [11,22]). A key difference in the behavior of the single shear and double shear configurations is the slip level at which the ultimate capacity occurs. It can be observed that in the double shear connections, the ultimate capacity occurs prior to a slip of 0.02-in of slip, similar to the behavior outlined by Case (a) in Figure 4.1. However, the single shear connections displayed a significantly lower slip stiffness (approximately 63% of double shear connections) and a behavior that resembles Case (c) in Figure 4.1 where the ultimate capacity is reached at slip deformations higher than 0.02-in. A previous study conducted by Bendigo et al. [12] indicated that the ultimate capacity of a bolted-only single shear connection was approximately one-half the ultimate capacity of a double shear connection constructed of

similar characteristics [12]. Analyzing the load-deformation response presented in Figure 5.4 and Figure 5.5, the ultimate capacity of the single shear combination connection is very close to one-half that of the ultimate capacity of double shear combination connections (approximately 48 %) even though the weld dimensions of the single and double shear tests are slightly different. However, in terms of the slip capacity (i.e., force at 0.02-in of slip), the single shear configuration resulted in a 60% reduction, on average, compared to the double shear configuration. This drop in the slip capacity and initial stiffness can be attributed to secondary bending that affects the behavior at small deformation levels.

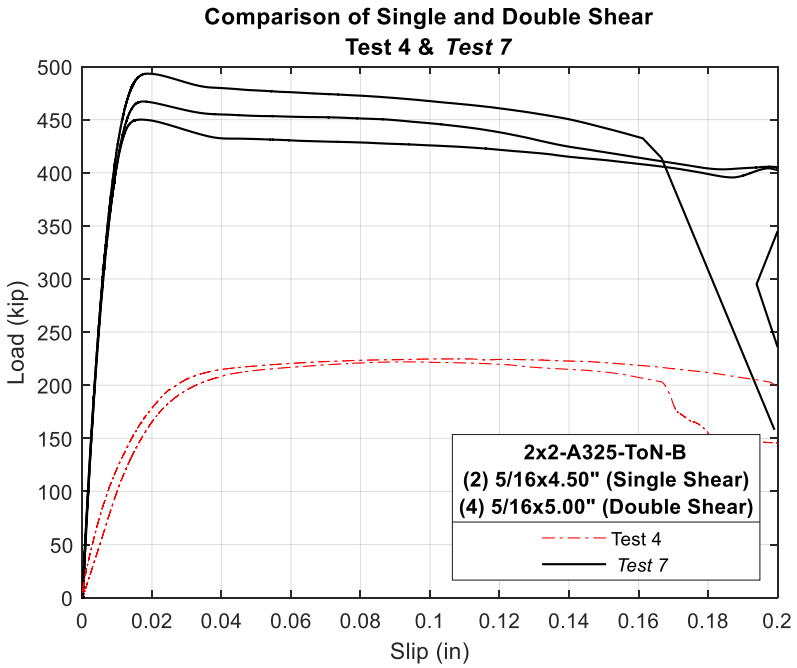

Figure 5.4: Comparison of Single Shear and Double Shear Testing

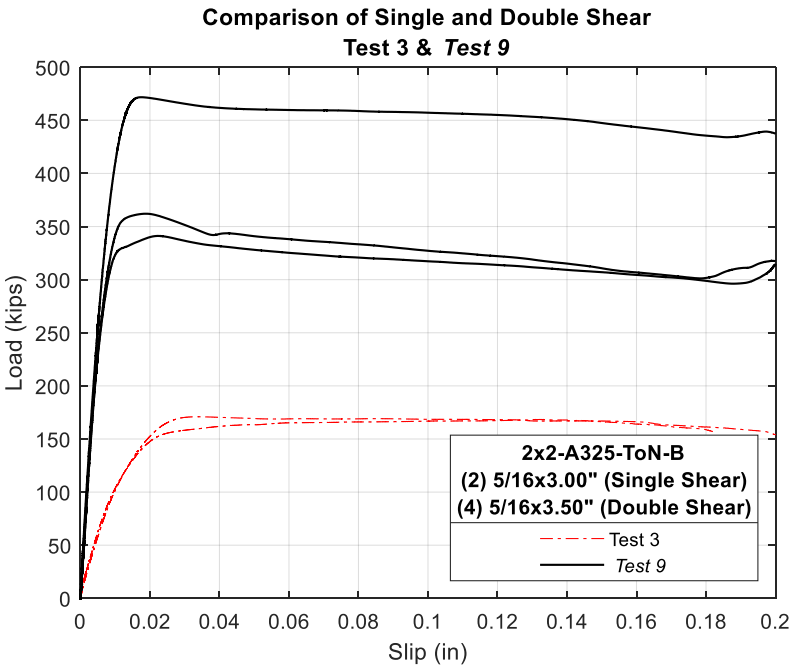

Figure 5.5: Comparison of Single Shear and Double Shear Testing

A comparison between the slip capacity and ultimate capacity of single shear and double shear testing is provided in Table 5.5 and Table 5.6. The results provided in Table 5.6 show an ultimate capacity of Test 4 (Single Shear) to be 47.5% the ultimate capacity of Test 7 (Double Shear). Additionally, the ultimate capacity of Test 3 (Single Shear) was 48.2% the capacity of Test 9 (Double Shear). To better understand the behavior of these connections and quantify the effect of key input parameters, a numerical investigation was conducted using Abaqus software as discussed in the next subsection of this thesis.

Table 5.5: Comparison of Single Shear and Double Shear Slip Capacity:

Test Configuration	Test Slip Capacity (kips)	Average (kips)	Single Shear/Double Shear
Test 3 - Single Shear (3" Weld)	152.51	150.07	42.7%
	147.64		
Test 9 - Double Shear (3.5" Weld) [Soliman et al. [11]]	340.00	351.05	
	362.10		
	471.7*		
Test 4 - Single Shear (4.5" Weld)	165.45	171.94	36.6%
	178.43		
Test 7 - Double Shear (5" Weld) [Soliman et al. [11]]	493.30	470.17	
	467.10		
	450.10		

*Excluded from average because it does not accurately represent the minimum capacity of the double shear configuration under this configuration.

Table 5.6: Comparison of Single Shear and Double Shear Ultimate Capacity

Test Configuration	Test Ult. Capacity (kips)	Average (kips)	Single Shear/Double Shear
Test 3 - Single Shear (3" Weld)	170.96	169.33	48.2%
	167.71		
Test 9 - Double Shear (3.5" Weld) [Soliman et al. [11]]	340.00	351.05	
	362.10		
	471.7*		
Test 4 - Single Shear (4.5" Weld)	222.04	223.45	47.5%
	224.86		
Test 7 - Double Shear (5" Weld) [Soliman et al. [11]]	493.30	470.17	
	467.10		
	450.10		

*Excluded from average because it does not accurately represent the minimum capacity of the double shear configuration under this configuration.

5.2.4 Finite Element Investigation

A finite element study of the 2x2 Class B axial lap steel connection with a single shear plane was conducted in order to supplement the results of the experimental testing program and provide a deeper understanding of the effect of underlying parameters. The results of the experimental testing exhibited out-of-plane bending in the tested connection that was proportional to the ultimate force carried by the connection. This bending effect was caused by the inherent eccentricity induced by the single shear plane under load. Figure 5.6 shows the bent plates of the specimen used for Test 4A after concluding the test. As shown in Figure 5.6, the bending in the connection may form a gap between the connected plates that alters the stress distribution along the weld and can be critical to the inner bolts of the connection. Accordingly, these single shear connections display a more complex behavior in experimental testing when an external bracing system is not applied. The finite element model was constructed to validate the load-deformation response collected from experimental testing and quantify the stresses that occur throughout the testing procedure. The remainder of this section will discuss the construction of the finite element model and load-deformation behavior compared to experimental results.

Figure 5.6: Image of Bending that occurred in Single Shear Splice Plate after Test 4A at Bert Cooper Lab in Stillwater, OK

5.2.4.1 Finite Element Model Assembly

Abaqus [31], a commercial finite element software, has been used to create and analyze the numerical model of the specimens. Figure 5.7 displays the three dimensional finite element model including all meshed parts within the assembly of a single shear lap connection. The assembly consists of four parts: a lower grip plate, tested bolts, weld lines, and splice plate. Each part is meshed using C3D8 elements. A C3D8 element is a linear brick element that consists of 8 nodes (i.e., a node at every corner of the brick). All parts are constructed based on the nominal dimensions of the test specimen. To improve the bending response of the model, the grip plate and splice plate are composed of elements with a seed length of approximately 0.35 the size of the global part. The

pretensioned bolt is simplified by omitting the shank and modeling the bolt using a solid disk in place of the head and nut with an approximate element seed length of 0.2 the size of the global part. Since the tested connections did not experience bearing, this was the best practice to ensure a consistent tension force throughout the simulation and that no interference between the bolt shank and edge of bolt holes would occur in the model. The weld is modelled as a triangular shape with leg sizes of 5/16-in and a total length of 4.5-in about the center of gravity of bolts. The meshing of the plates and bolts are the same. However, a finer mesh is used on the welded parts with an element seed length of approximately 0.05 the size of the global element. This allows for more refined analysis of stresses along the weld line.

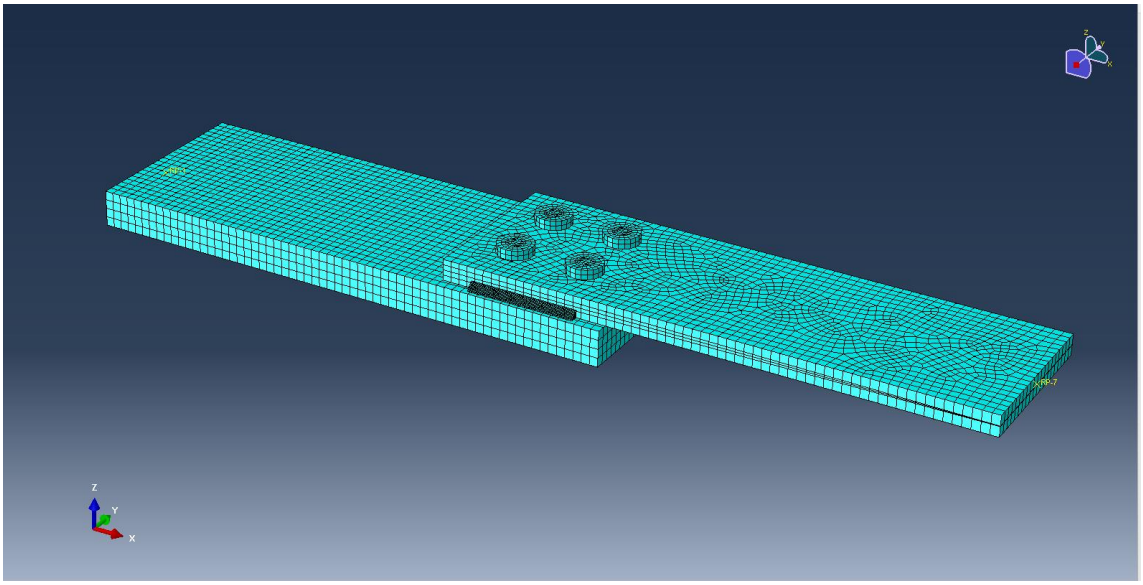

Figure 5.7: Abaqus Finite Element Model with Mesh

5.2.5 Material Properties

The material properties used in the finite element model were gathered from the AISC [2,7]. The bolts and plates were modelled according to the characteristics of an A325 bolt and A572 plate provided by AISC [2,7]. Additionally, the weld was modelled with a yield stress of 80 ksi. This was estimated from previous work by [11,22] which noted a weld shear stress range of 47.4-55.1 ksi. The yield stress corresponding to this shear stress range should be 79.0-91.8 ksi, and a value of 80.0 ksi was chosen for the yield stress in this simulation.

5.2.5.1 Contact Interactions

In connections similar to the ones modelled herein; it is critical to properly define surface contact interactions within the finite element simulation. In this model, all surface interactions have been defined manually as *General Contact* in Abaqus. A *General contact* interaction in Abaqus is used with a *Surface-to-surface* and a *Finite sliding* procedure to properly characterize the contact behavior. The tangential contact behavior is assumed f*rictionless* for all areas that occur outside the faying surface of the slip-critical single shear lap splice. The interaction between slip surfaces of the connection is formulated by using the penalty method with a user defined friction coefficient of 0.44, which is similar to the slip coefficient found in experimental testing by [22]. This experimental work by [22] also displayed a high variance in the slip coefficient ranging from 0.414-0.636 in Class B faying surfaces.

5.2.5.2 Boundary Conditions and Simulation

Proper boundary conditions must be applied so the desired behavior is gathered from the finite element model. In this case, the end of the splice plate is fixed against translation

and rotation as the load procedure begins. Additionally, the end of the grip plate is free to translate and rotate about all axes. The boundary condition at the end of the grip plate also allows for a longitudinal displacement up to 0.26-in.

The finite element simulation is split into two steps. The first covers the application of the pretension load, next, the external load (or displacement) is applied. The pretension force is applied based on the average pretension force of 42.73 kips per bolt, the average pretension for a A325 ¾-in bolt in [22]. The force is applied to the surface of the four tested bolts on both sides of the connection. Next, the external displacement is applied to the connection similar to the monotonic loading procedure used in experimental testing. To accomplish this load procedure, the support at the end of the lower grip in the Abaqus model is released and displaced to 0.26-in in the longitudinal direction. Figure 5.8 shows the Abaqus model assembly without meshing.

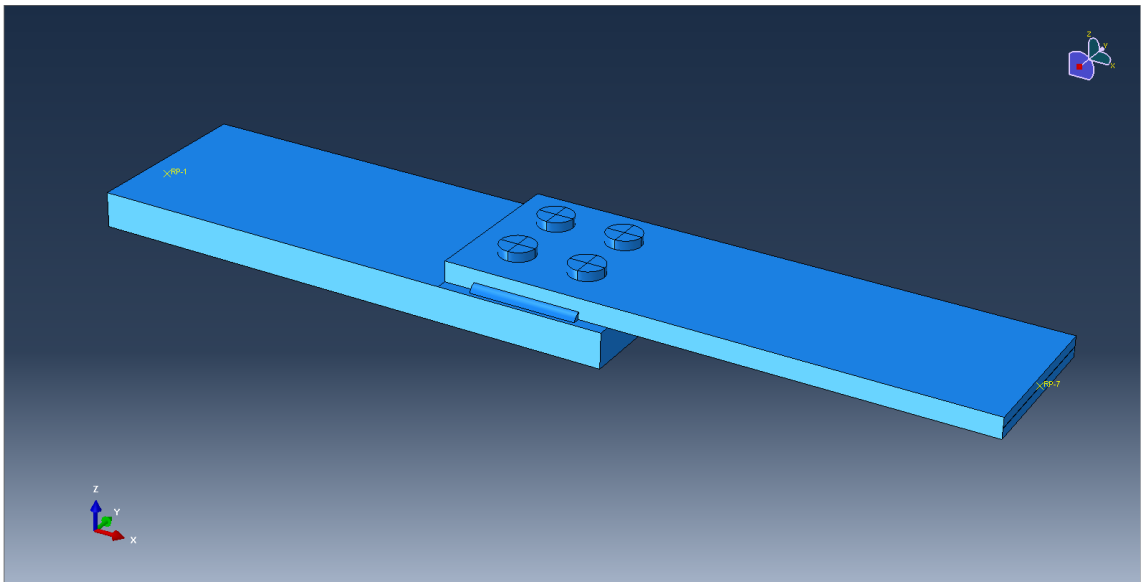

Figure 5.8: Abaqus Finite Element Model with applied Boundary Conditions

5.2.5.3 Finite Element Results

Figure 5.9 displays the load-deformation results of the finite element model compared to the experimental results of the bolted-only, welded-only, and combination tests. Overall, the load-deformation behavior of the finite element model follows closely that of the experimental data, especially for the combination connections. The use of the finite element model gives very close estimates to both the slip capacity and the ultimate capacity for the considered tests. However, it some differences are observed in the ultimate capacity of the welded-only test. However, it is important to note the dimensions of the weld in the finite element model are based on the nominal leg size and length of the weld in the testing matrix. The actual built dimensions of the weld vary slightly and may have resulted in the difference we observe in the welded-only test of Figure 5.9 (b).

After the finite element model was validated with experimental test results, two parametric studies on plate thickness and weld length were performed to quantify their influence on the behavior of a single shear axial lap splice connections.

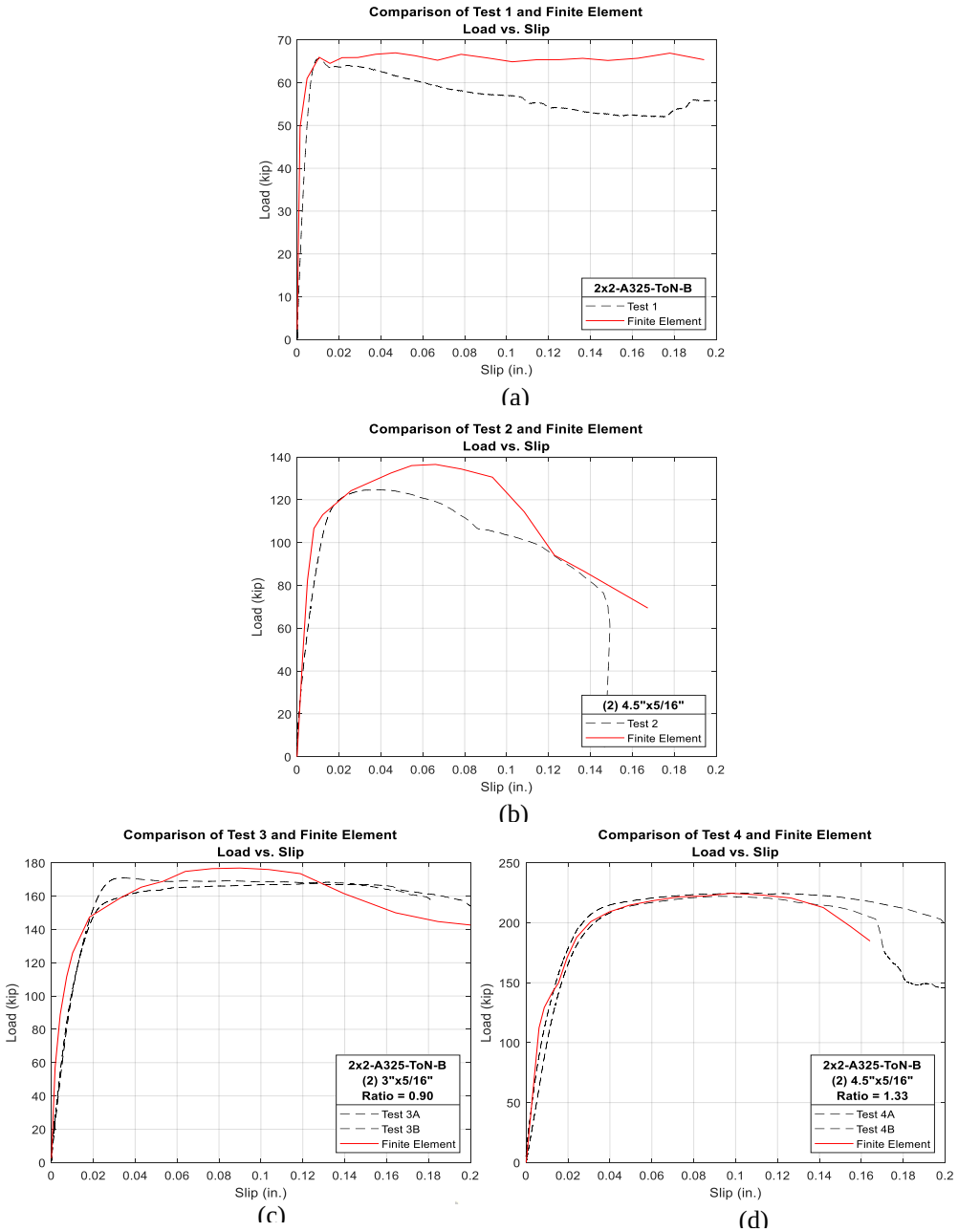

Figure 5.9: Figure 1.9: Comparison of Experimental and Finite Element Results (a) Bolted-Only (b) Welded-Only (c) Combination Test 3 (d) Combination Test 4

5.2.5.4 Effect of Plate Thickness on the Load-Deformation Behavior

Three finite element models were constructed with the only difference being the thickness of the splice plate. Models with a splice plate thickness of ¾-in and 1”-in were

created, and a 7/8-in splice plate thickness was adopted from validated model of the experimental test. Figure 5.10 shows the load-deformation profiles for the three models. The results show little effect to both the slip capacity and ultimate capacity on the load-deformation behavior of the connection when altering the thickness of the splice plate.

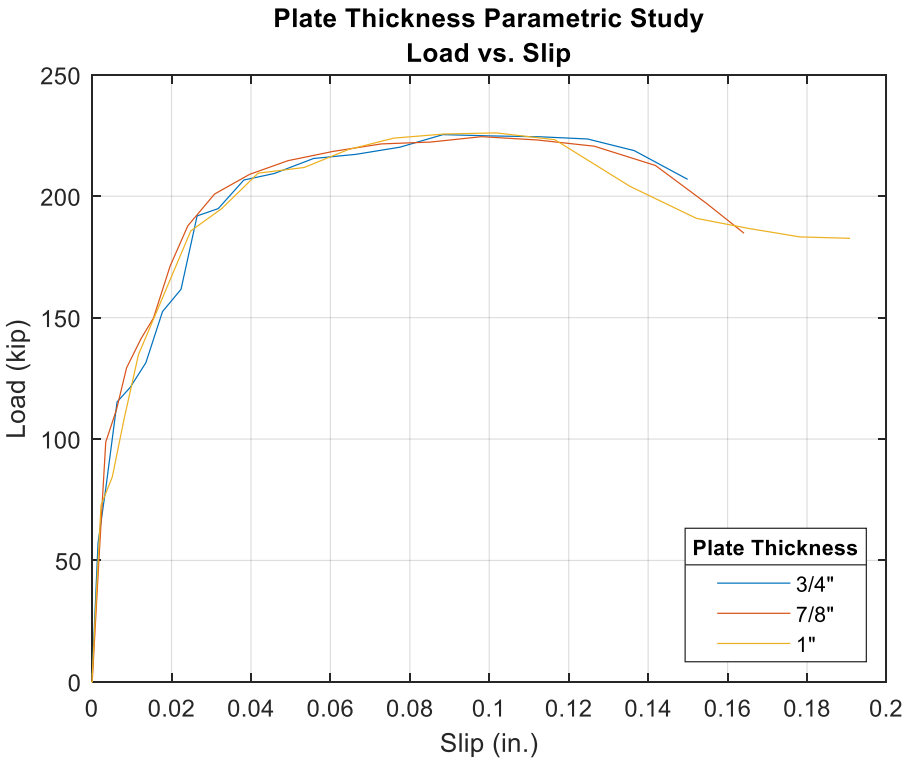

Figure 5.10: Plate Thickness Parametric Study

5.2.5.5 Effect of Weld Length on the Load-Deformation Behavior

The second parametric investigation was performed to quantify the effect of weld length on the load-deformation behavior of the single shear axial lap splice connection with bolts and welds in combination. Each model was constructed with a weld about the bolt center of gravity with the same root geometry of the weld and varying weld lengths (1.5-in,3-in,4.5-in, and 6-in). Figure 5.11 displays the results of the investigated models. As

shown in the figure, an increase in the stiffness, slip capacity, and ultimate capacity is achieved when the weld length is increased.

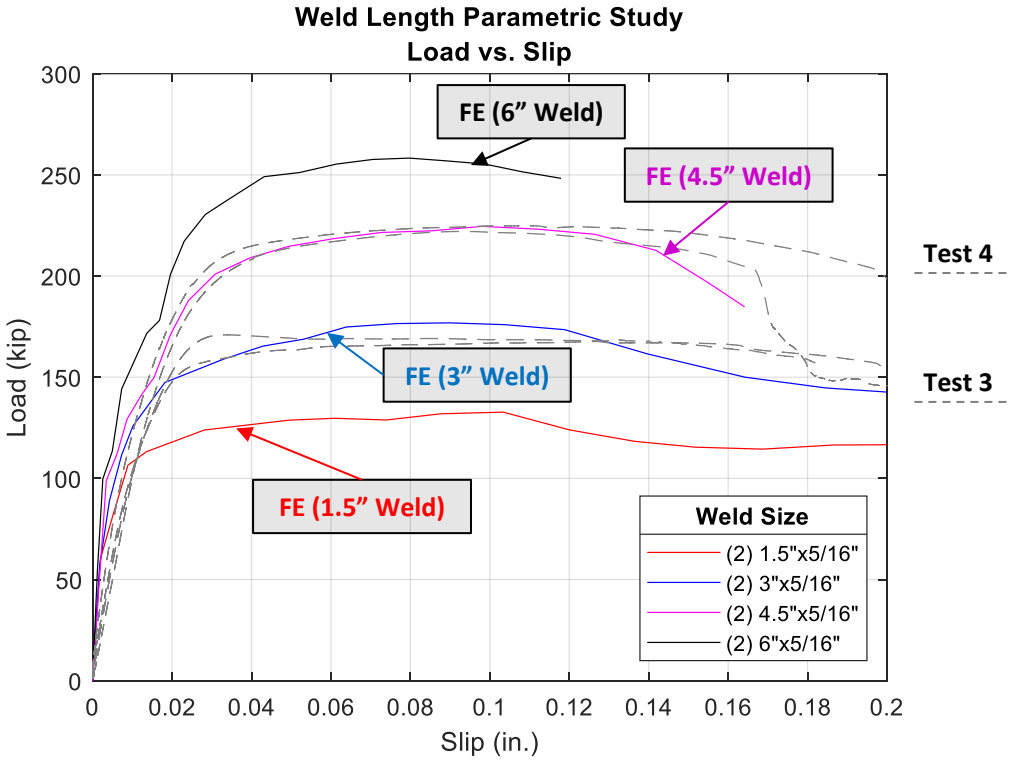

Figure 5.11: Weld Length Parametric Study

Table 5.7 lists the slip and ultimate capacity of the modeled connections in comparison to the As-Built prediction model. In Table 5.7 the As-Built capacity was calculated based on the same nominal dimensions used to construct the finite element model. Since the As-Built was created to predict a capacity based on the measured mechanical characteristics of the connecting fasters, it gives a very close prediction to the finite element results.

Table 5.7: Comparison of Finite Element and As-Built prediction

Test	Weld/Bolt Ratio	Test Slip Capacity (kips)	Test Ult. Capacity (kips)	As-Built Prediction	Test Slip/As-Built	Test Ult./As-Built
FE (1.5" Weld)	0.45	117.94	132.73	137.38	0.86	0.97
FE (3" Weld)	0.90	148.80	176.85	183.31	0.81	0.96
FE (4.5" Weld)	1.33	172.55	224.54	229.24	0.75	0.98
FE (6" Weld)	1.75	202.75	258.28	275.18	0.74	0.94

5.2.6 Assessment of the AISC Prediction Model

All test results were compared to the AISC predicted capacity to quantify a factor of safety for each test in the experimental program. The AISC capacity, AISC R_n, is calculated as the direct addition of strength provided by the bolts and welds, respectively. The R_n capacity for each fastener is calculated from Eq. 3 and Eq. 6 provided in Chapter 2. The following sections will investigate the factor of safety of the AISC prediction model against the slip capacity and ultimate capacity of single shear experimental data.

5.2.7 AISC Prediction Model Compared to Single Shear Ultimate Capacity

Table 5.8 provides the ultimate test capacity, AISC R_n prediction, and the factor of safety calculation while Figure 5.12 plots the AISC factor of safety. As seen in the table, the ultimate capacity for each of the experimental tests outperformed the AISC R_n prediction

model by a factor of 1.33-1.68. However, the bolted-only result was an exception to this finding. The bolted-only case barely surpassed the AISC capacity prediction, having a factor of safety of 1.04. Note that the AISC prediction model uses the nominal friction coefficient and bolt pretension force. A higher safety factor was expected using these values given the higher values of actual pretension force and friction coefficient found in [11,22]. This drop in capacity could be due to the variability associated with Class B bolted-only connections that was observed in [11]. However, with only a single test result, it is difficult to draw conclusive statements based on the recorded behavior. Accordingly, additional testing on bolted-only single shear connections is recommended to better understand its load-deformation behavior.

Table 5.8: Factor of Safety Calculation based on AISC prediction model and Experimental Ultimate Capacity

	Test No	AISC R_n (kips)	Test Ult. Capacity (kips)	Test Ult./AISC R_n	Average	SD`	COV	
Bolted-Only	1	63.30	65.61	1.04	---	---	---	
		---	---	---	---	---	---	
Welded-Only	2	83.50	124.72	1.49	---	---	---	
Combination (Bolts + Welds)	3	119.00	170.96	1.44	1.423	0.019	1.358%	**AVG = 1.503 SD = 0.1 CV = 6.677%**
		119.00	167.71	1.41				
	4	146.80	222.04	1.51	1.522	0.014	0.892%	
		146.80	224.86	1.53				
	5	146.80	212.26	1.45	1.515	0.097	6.421%	
		146.80	232.45	1.58				
	6	146.80	221.06	1.51	1.593	0.124	7.772%	
		146.80	246.77	1.68				
	7	146.80	195.93	1.33	1.460	0.177	12.126%	
		146.80	232.68	1.59				
SD = Standard Deviation; COV = Coefficient of Variance								

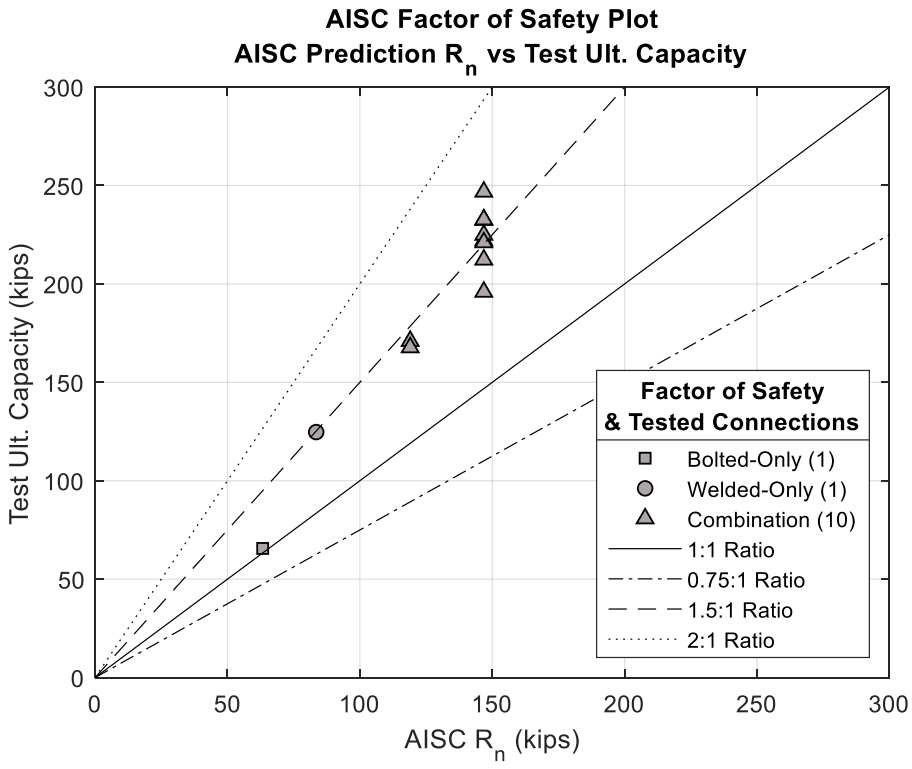

Figure 5.12: AISC Factor of Safety plot based on Ultimate Capacity

5.2.8 AISC Prediction Model Compared to Single Shear Slip Capacity

Since these connections can be in essence slip-critical joints, it may be desirable to limit the slip of the connection under service or ultimate loads. Accordingly, it is essential to quantify their experimental slip capacity to nominal capacity prediction of the AISC. Table 5.9 displays the slip capacity, nominal AISC R_n capacity, and the factor of safety calculations. As discussed above in this thesis, the single shear combination connections are characterized by a lower initial slip stiffness and undergoe gradual slip throughout the test. As a result, the recorded slip capacities are significantly lower than the ultimate capacity discussed in the previous section. The factor of safety exceeded 1.13 in all tests

except a single specimen of Test 7 that had a safety factor of 0.95. As noted in section 5.2.2, high variability was observed when completing the welds prior to pretensioning the bolts. If we factor out the results of Test 7, the corresponding safety factor of the AISC prediction model for a slip critical connection design would range from 1.13-1.39. The results of the factor of safety calculations for the AISC model compared to the slip capacity of tested connections is provided in Figure 5.13. Again, it should be noted that the values in Table 5.8 were based on the nominal design parameters of connecting elements. Accordingly, these results may not provide a clear picture on the accuracy of the AISC model in predicting the capacity of the connection. Accordingly, it is necessary to quantify the accuracy of the AISC model using the material properties obtained from ancillary testing. This analysis is discussed next.

Table 5.9: Factor of Safety Calculation based on AISC prediction model and Experimental Slip Capacity

	Test No	AISC R_n (kips)	Test Slip Capacity (kips)	Test Slip/AISC R_n	Average	SD	COV	
Bolted-Only	1	63.30	65.61	1.04	---	---	---	
		---	---	---	---	---	---	
Welded-Only	2	83.50	---	---	---	---	---	
Combination (Bolts + Welds)	3	119.00	152.51	1.28	1.261	0.029	2.295%	**AVG = 1.219 SD = 0.13 CV = 10.687%**
		119.00	147.64	1.24				
	4	146.80	165.45	1.13	1.171	0.063	5.340%	
		146.80	178.43	1.22				
	5	146.80	169.67	1.16	1.162	0.009	0.793%	
		146.80	171.59	1.17				
	6	146.80	204.76	1.39	1.394	0.001	0.104%	
		146.80	204.46	1.39				
	7	146.80	140.00	0.95	1.109	0.219	19.757%	
		146.80	185.47	1.26				

SD = Standard Deviation; COV = Coefficient of Variance

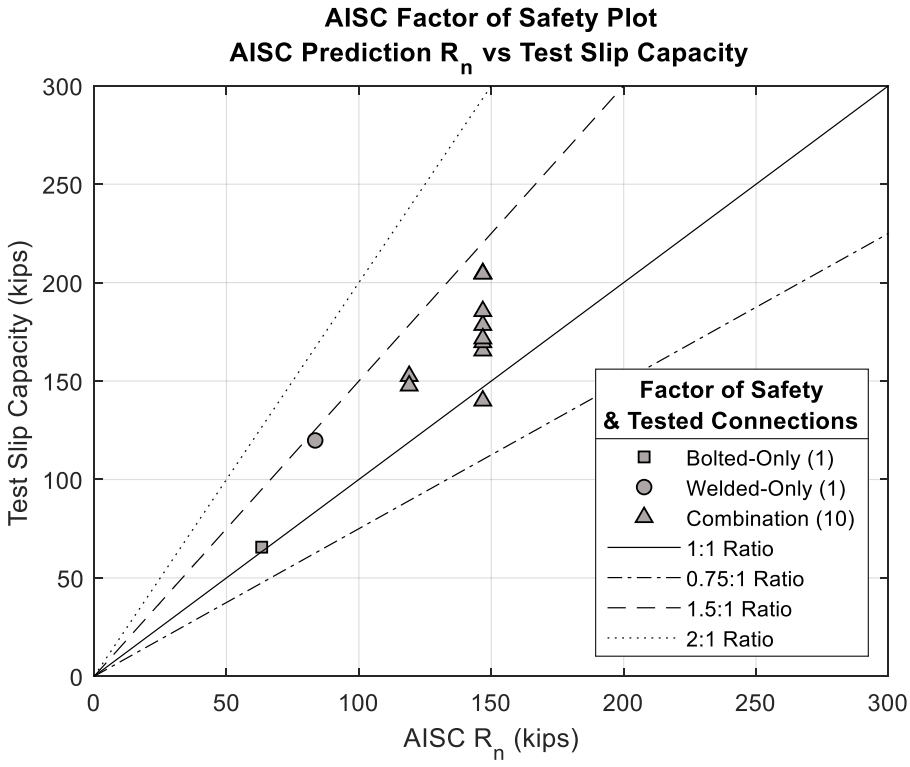

Figure 5.13: AISC Factor of Safety Plot based on Slip Capacity

5.2.9 As-Built Prediction

All test results were compared to the As-Built predicted capacity to quantify a factor of safety for each test in the experimental program. The As-Built capacity, As-Built R_n, is calculated as the direct addition of strength provided by the bolts and welds, respectively. The method of calculating the As-Built prediction has been provided in Section 4.3. The following sections will investigate the factor of safety of the As-Built prediction model against the slip capacity and ultimate capacity of single shear experimental data.

5.2.10 As-Built Prediction Compared to the Single Shear Ultimate Capacity

The As-Built prediction, ultimate test capacity, and the safety factor of the tested connections is provided in the Table 5.10. As seen in the table, the As-Built prediction for

the bolted-only single shear case resulted in a factor of safety of 0.70. This reduced test capacity may be attributed to the bending that occurred in the single shear specimen which could form a gap between the connected plates. However, as indicated above, more testing is recommended to enable a better prediction of the behavior. The As-Built prediction for the welded-only single shear test resulted in a factor of safety of 0.97. This factor of safety is very close to 1.0 and indicates that the As-Built prediction can very closely predict the ultimate capacity of a welded only test.

Lastly, the factor of safety for the 10 combination test ranged from 0.93 to 1.22 with the average factor of safety being 1.018. The results of Test 3,4,5, and 7 display an ultimate capacity similar to the capacity of the As-Built prediction model, which produces a factor of safety ranging from 0.93-1.07. Test 6B displays the highest factor of safety, 1.22. As noted in Section 5.2.1, Test 6 experienced a gain in strength which is attributed to the change in fracture angle of the weld. The variance that does exist can be partially attributed to the nature of the testing matrix which altered the location of the weld and installation technique. An illustration of the factor of safety calculations for the As-Built model compared to the ultimate capacity of tested connections is provided in Figure 5.14.

Table 5.10: Factor of Safety Calculation based on As-Built prediction model and Experimental Ultimate Capacity

	Test No	As-Built R_n (kips)	Test Ult. Capacity (kips)	Test Ult./As-Built R_n	Average	SD	COV	
Bolted-Only	1	94.08	65.61	0.70	---	---	---	
		---	---	---	---	---	---	
Welded-Only	2	128.38	124.72	0.97	---	---	---	
Combination (Bolts + Welds)	3	180.21	170.96	0.95	0.940	0.012	1.295%	**AVG = 1.018 SD = 0.093 CV = 9.12%**
		180.05	167.71	0.93				
	4	234.11	222.04	0.95	1.013	0.091	9.028%	
		208.63	224.86	1.08				
	5	218.77	212.26	0.97	1.001	0.044	4.366%	
		225.23	232.45	1.03				
	6	210.18	221.06	1.05	1.138	0.122	10.713%	
		201.58	246.77	1.22				
	7	211.04	195.93	0.93	0.999	0.101	10.055%	
		217.35	232.68	1.07				
SD = Standard Deviation; COV = Coefficient of Variance								

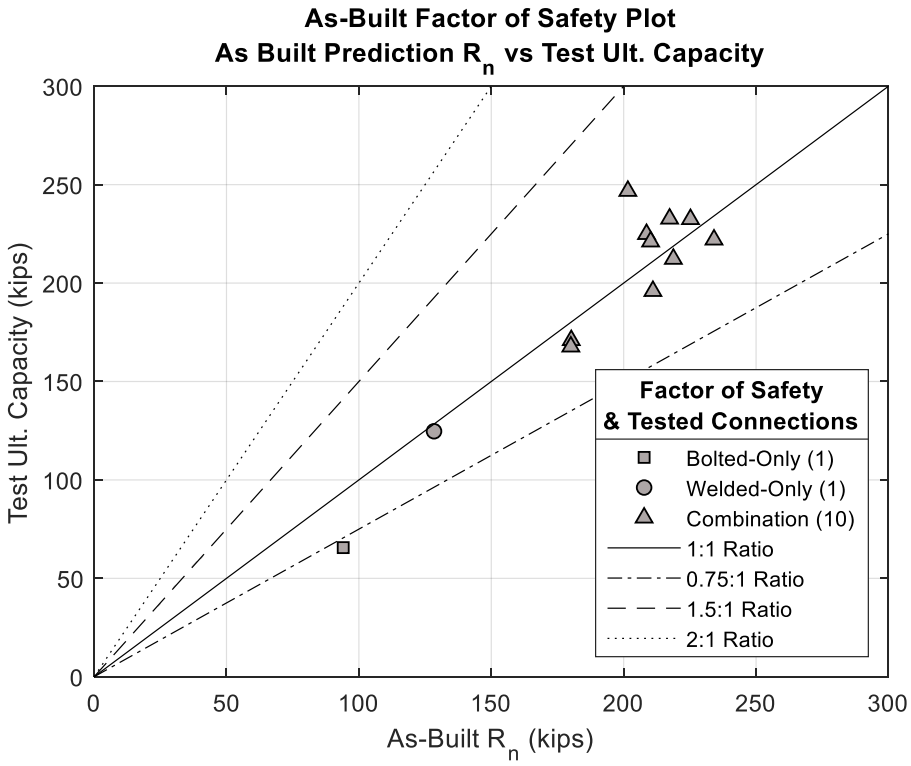

Figure 5.14: As-Built Factor of Safety Plot based on Ultimate Capacity

5.2.11 As-Built Prediction Compared to the Single Shear Slip Capacity

Table 5.11 shows the As-Built prediction, experimental slip capacity, and safety factor of the tested connections. Figure 5.15 plots the results of the factor of safety calculations for the bolted-only, welded-only and combination tests with respect to the As-Built prediction. This comparison, which is crucial for the proper design of a slip-critical connections, shows that the factors of safety ranges from 0.66 to 1.01 with an average of 0.827. Accordingly, it is evident that the As-Built prediction model cannot accurately predict the slip load of the single shear connections. To maintain a reliability level similar to that of double shear combination connections, the estimate of the slip capacity of single shear combination connections should be reduced to account for the lower slip stiffness of these connections.

Table 5.11:Factor of Safety Calculation based on As-Built prediction model and Experimental Slip Capacity

	Test No	As-Built R_n (kips)	Test Slip Capacity (kips)	Test Slip/As-Built R_n	Average	SD	COV	
Bolted-Only	1	94.08	65.61	0.70	---	---	---	
		---	---	---	---	---	---	
Welded-Only	2	128.38	119.83	0.93	---	---	---	
Combination (Bolts + Welds)	3	180.21	152.51	0.85	0.833	0.019	2.232%	**AVG = 0.827 SD = 0.109 CV = 13.17%**
		180.05	147.64	0.82				
	4	234.11	165.45	0.71	0.781	0.105	13.449%	
		208.63	178.43	0.86				
	5	218.77	169.67	0.78	0.769	0.010	1.265%	
		225.23	171.59	0.76				
	6	210.18	204.76	0.97	0.994	0.028	2.850%	
		201.58	204.46	1.01				
	7	211.04	140.00	0.66	0.758	0.134	17.710%	
		217.35	185.47	0.85				
SD = Standard Deviation; COV = Coefficient of Variance								

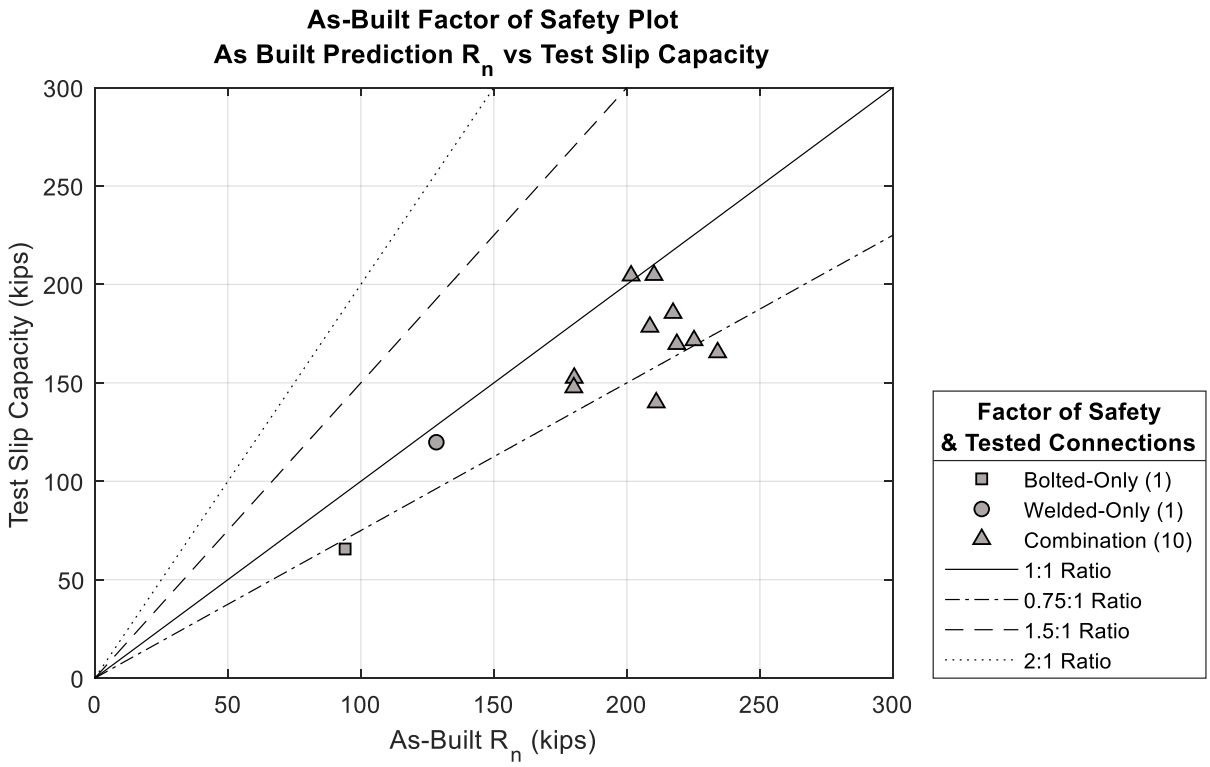

Figure 5.15: As-Built Factor of Safety Plot based on Ultimate Capacity

5.3 DISCUSSION OF FATIGUE TESTING RESULTS

5.3.1 Specimen Cracking

During the fatigue testing, it was evident the combination connection possessed a significant fatigue reserve capacity beyond the first event of crack initiation. In Test F1, the connection did not experience any cracks until 436,799 cycles were recorded. At this point, the connection had surpassed AASHTO Category D (275,000 cycles) requirements using the gross cross-sectional area for calculating the stress. The initial crack in the connection can be observed in 5.16 (a).

After the initial cracking formed, three additional cracks in the connection had been observed for a total of 4 cracks before a crack had reached the first bolt hole. At this point, the fatigue test had undergone approximately 774,773 cycles. A crack forming from the edge of the plate to the bolt hole was the failure criteria set in testing by Bowman [20]. However, since the connection still maintained an adequate stiffness level to hold the maximum capacity of the fatigue loading, the test was continued. The crack propagation to the edge of the bolt hole can be seen in Figure 5.16 (b).

The test was continued for another 571,830 cycles before a crack was observed on the inner half of the bolt hole at a total of 1,346,603 cycles. This crack can be observed in Figure 5.16 (c). Finally, at 1,399,748 cycles the connection experienced a complete loss of stiffness when a fracture occurred across an entire splice plate in the double shear connection. This fracture can be observed in Figure 5.16 (d). A larger view of the final fracture is provided in Figure 5.17.

Figure 5.16: Fatigue Test Specimen after Failure

Figure 5.18 displays the global stiffness of the tested connection at different number of cycles. The figure also shows the cracking milestones and the limits for fatigue service life based on different AASHTO detail categories [8]. The stiffness plotted in Figure 5.18 represents the global system stiffness since is computed from the load and displacement readings of the MTS actuators. Accordingly, it includes the elongation of the entire specimen, as well as deflections of the upper and lower header beams. The

cracking milestones indicated are: Initial cracking, first crack to reach bolt hole, crack reaches center of plate, and loss of stiffness. As seen from the figure, during the fatigue test, the connection maintained its stiffness until a fracture of the splice plate occurred. Although the end is illustrated as a steep drop in Figure 5.13, the connection underwent a gradual loss in stiffness until a fracture occurred in the splice plate.

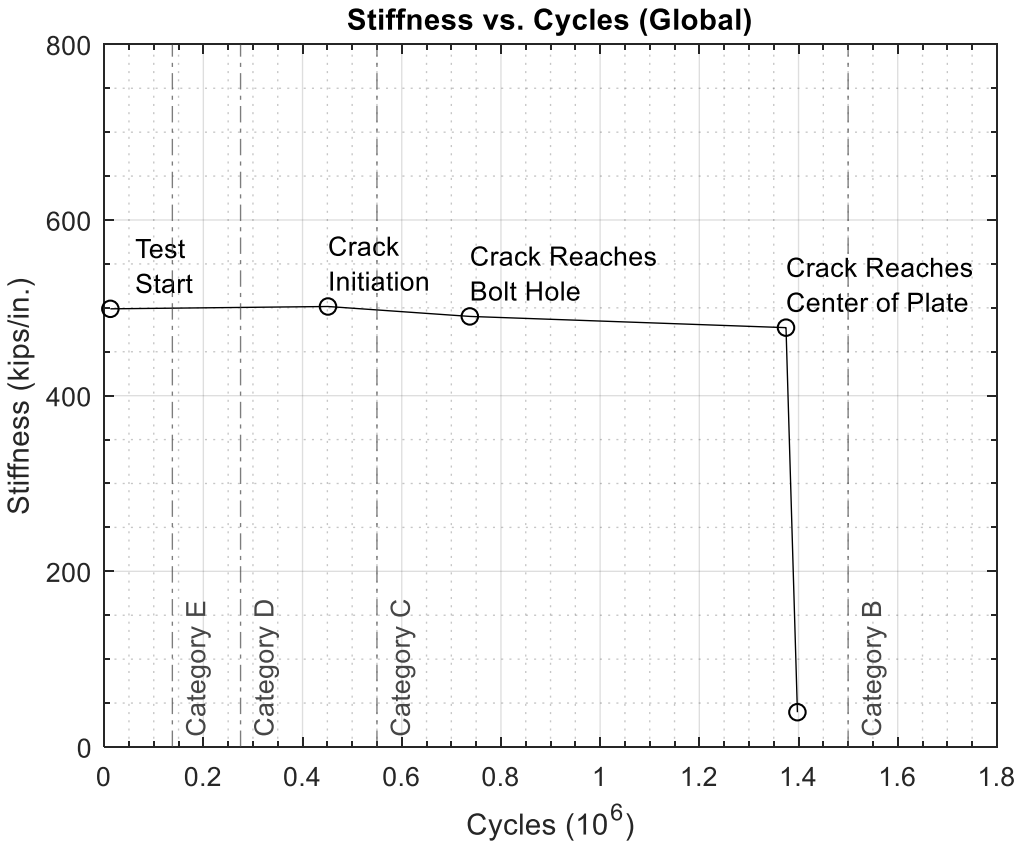

Figure 5.17:Effective stiffness of the Global System at different stages of Cracking

Figure 5.18 also provides a good indication of how the connection behaved with respect to the fatigue categories established by the AASHTO *LRFD Bridge Design Specification* [8]. The initial cracking in the connection was observed in the area that would have classified this detail in Category D. However, the crack did not extend from the edge of

the plate to the first bolt hole until it had already propagated well into the region of Category C. The test specimen experienced a loss of stiffness within the limits of Category C as well. This result is consistent with the findings in [20], which concluded that riveted connections with tack welds can follow the fatigue service life established by detail Category C [20].

CHAPTER VI

6 SUMMARY AND CONCLUSIONS

6.1 SUMMARY

This research study has been conducted to provide a greater depth of knowledge on the behavior of axial lap steel connections with bolts and welds in combination. To accomplish this, 12 single shear axial lap splice connections have been tested under monotonic tensile loading and one test has been performed to characterize the fatigue behavior of a double shear combination connection. The experimental testing program investigated the slip capacity, ultimate capacity, and fatigue life of combination connections. Additionally, variables in the direct tension testing were altered to better understand their influence on combination connection performance. The parameters included: weld/bolt ratio, weld location with respect to bolts and connecting elements installation sequence. The influence of variables was discussed and the experimental results were compared to the AISC prediction as well as the As-Built prediction. The results of fatigue were also compared to previous research and the AASHTO fatigue categories.

6.2 CONCLUSIONS

- The following conclusions can be drawn from this study: The ultimate capacity of the single shear combination connections exceeded the AISC prediction (AISC R_n) when nominal mechanical properties of connecting elements are used. The safety factor ranged from 1.33-1.68. Therefore, it is conservative to use the AISC prediction model when predicting the ultimate capacity of single shear combination connections. Using the measured mechanical properties of connecting elements (i.e., the As-Built prediction model) provided very accurate prediction of the ultimate capacity of the single shear combination connection.
- The slip capacity of the single shear combination connections exceeded the AISC prediction (AISC R_n) by a factor of 1.13-1.39 (excluding Test 7) when nominal mechanical properties are used. However, when the measured mechanical properties are used (i.e., the As-Built prediction), the current models fail to provide a conservative estimate of the slip load. This under conservatism reached 29% for some specimens tested herein. Accordingly, to maintain a proper reliability level of single shear combination connections against slip, it is recommended that prediction models should be modified to reflect this drop in capacity.
- The single shear combination connection provided an ultimate capacity that was approximately one-half that of the double shear combinations connections of similar configuration. However, the initial stiffness of the single shear configuration is significantly lower than that of double shear combination connections. This can be attributed to the effect of secondary bending that occurs in single shear connections.

- The results of experimental testing show the slip capacity, ultimate capacity, and stiffness of a single shear combination connection can be increased by placing the welds in a location to prevent the separation of plates caused by bending.
- It is recommended to pretension the bolts prior to installing welds on combination connections. Connections constructed with welding first may contain gaps along the slip surface that can prevent the bolts from reaching their full slip capacity and produce a higher variance in the slip capacity and ultimate capacity performance.
- Based on the conducted numerical analysis, plate thickness did not have a significant effect on behavior of single shear combination connections. However, the analysis did not cover other shapes of steel members (e.g., angles or t-shaped members).
- Under fatigue loading the tested combination connection possessed ample fatigue life to be considered as a detail under AASHTO Category C.

6.3 FUTURE WORK

Since a limited amount of experimental work was performed in this study, several recommendations for future work have arisen in the process. These recommendations include the following:

- Additional bolted-only single shear testing is needed to characterize the variability in the slip behavior of single shear axial lap joints.
- Additional large-scale experimental testing to investigate the influence of the faying surface class on both the load-deformation behavior of combination

connections with a single shear plane and fatigue life of double shear combination connections

- An experimental program organized to better understand the behavior of combination connections under low cycle loading to evaluate the seismic performance of combination connections
- Additional testing of single shear combination connections with varied bolt hole configurations
- Additional investigations on the effect of more connection attributes (e.g., number of bolt rows and dimensions of the splice plate) on the load-deformation behavior of the single shear connections.
- Testing and finite element analysis are required to quantify the behavior of single shear connections made with steel members other than flat plates (e.g., angles or t-shaped members)

REFERENCES

[1] Fisher, J.W., and Struik, J. H. A., 1973. *Guide to Design Criteria for Bolted and Riveted Joints*. New York, NY: John Willey and Sons. Inc.

[2] AISC, 2016. *Specification for Structural Steel Buildings*, ANSI/AISC 360-16. Chicago, IL: American Institute of Steel Construction.

[3] Quinn, B.P., 1991. *The effect of profile and root geometry on the strength of fillet welds*, M.Sc. Thesis. Department of Civil Engineering, Purdue University, West Lafayette, IN.

[4] Godfrey, H.J., and Mount, E.H., 1940. Pilot tests on covered electrode welds, *Welding Journal*, 19, Reprint No. 48 (40-2).

[5] Higgins, T.R and Preece, F.R., 1969. Proposed working stresses for fillet welds in building Construction. *Engineering Journal*, AISC, 6(1), 16-20.

[6] Fisher, J.W., Ravindra, M.K., Kulak, G.L., and Galambos, T.V., 1978. Load and resistance factor design criteria for connectors. *Journal of the Structural Division*, 104(9), 1427-1441.

[7] AISC, 2017. *Steel Construction Manual*, 15th Edition. Chicago, IL: American Institute of Steel Construction, Inc.

[8] AASHTO, 2020. *LRFD Bridge Design Specifications*, 9th ed. Washington, D.C.: American Association of State Highway and Transportation Officials.

[9] Holtz, N.M. and Kulak, G.L., 1970. *High-strength bolts and welds in load-sharing systems, Structural Engineering Report No. 8*. Department of Civil Engineering, Nova Scotia Technical College, Halifax, Nova Scotia.

[10] Jarosch, K. H. and Bowman, M. D., 1986. Tension Butt Joints with Bolts and Welds, *Engineering Journal*, AISC, 23(1), 25-35.

[11] Soliman, M., Russell, B., Waite, C. W., Shen, L., and Stringer, E., 2021. *The Behavior of Steel Connections with Bolts and Welds in Combination*, Report prepared for The American Institute of Steel Construction. School of Civil and Environmental Engineering, Oklahoma State University, Stillwater, OK. Report submitted for publication.

[12] Bendigo, R. A., Fisher, J. W., and Rumpf, J. L., 1962. *Static tension tests of bolted lap joints* (No. 271.9), Fritz Engineering Laboratory Report, Lehigh University, Bethlehem, PA.

[13] Shoukry, Z., and Haisch, W. T., 1970. Bolted connections with varied hole diameters. *Journal of the Structural Division*, 96(6), 1105-1118.

[14] Heistermann, C., 2011. *Behaviour of Pretensioned Bolts in Friction Connections - Towards the Use of Higher Strength Steels in Wind Towers,* Thesis. Department of Civil, Environmental and Natural Resources Engineering, Lulea University of Technology, Lulea, Sweden.

[15] Zhao, L., Xin, A., Liu, F., Zhang, J., and Hu, N., 2016. Secondary bending effects in progressively damaged single-lap, single-bolt composite joints, Results in Phys. 6. 704-711.

[16] Keating. P. B. and Fisher, J. W., 1986. *Review of Fatigue Tests and Design Criteria on Welded Details*, National Cooperative Highway Research Program Report 286, 86-21, Fritz Engineering Laboratory, Lehigh University, Bethlehem, PA.

[17] Ypeij, E., 1972. *New Development in Dutch Steel Bridge Buildings*, Preliminary Report 9th Congress IABSE. Amsterdam.

[18] Brown, J. D., Lubitz D. J., Cekov Y. C., Frank K. H., and Keating P. B., 2007. *Evaluation of Influence of Hole Making Upon the Performance of Structural Steel Plates and Connections*. Report No. FHWA/TX-07/0-4624-1. Center for Transportation Research, University of Texas at Austin, Austin, TX.

[19] Huhn, H. and Valtinat, G., 2004. *Bolted Connections with Hot Dip Galvanized Steel Members with Punched Holes*, Amsterdam: European Convention for Constructional Steelwork/American Institute of Steel Construction.

[20] Bowman, M. D., Fu, G., Zhou, Y. E., Connor, R. J., and Godbole, A. A., 2012. *Fatigue Evaluation of Steel Bridges*. National Cooperative Highway Research Program Report 721, Transportation Research Board, Washington, D.C.

[21] Sullivan, T.J., Calvi, G.M., and Priestley, M.J.N., 2004. *Initial Stiffness versus Secant Stiffnesss in Displacement Based Design* (Paper No. 2888). 13th World Conference on Earthquake Engineering, Vancouver, B.C., Canada.

[22] Waite, C.W., 2019. *Understanding the Behavior of Double Shear Axial Lap Steel Connections Made in Combination of Slip-Critical Bolts and Longitudinal Fillet Welds*, M.Sc. Thesis. School of Civil and Environmental Engineering, Oklahoma State University, Stillwater, OK.

[23] Kulak, G.L., and Grondin, G.Y., 2003. Strength of joints that combine bolts and welds. *Engineering Journal*, AISC, 40(2), 89-98.

[24] Shi, Y., Wang, L., Wang, Y., Ma, J., & Bai, R., 2011. Finite element analysis of the combined connection with bolts and welds. *Applied Mechanics and Materials*, 94- 96, 316-321.

[25] Shi, Y., Wang, L., Wang, Y., Ma, J., & Bai, R., 2011. Proposed design method of combined connections with bolts and longitudinal welds. *Applied Mechanics and Materials*, 94-96, 923-928.

[26] Fisher, J.W., 1964. *On the Behavior of Fasteners and Plates with Holes* (No. 288-18). Fritz Engineering Laboratory Report, Lehigh University, Bethlehem, PA.

[27] Salmon, C.G., Johnson, J.E., and Malhas, F.A., 2009. *Steel Structures: Design and Behavior: Emphasizing Load and Resistance Factor Design*. Upper Saddle River, NJ: Person Education.

[28] RCSC, 2014. *Specification for Structural Joints Using High-Strength Bolts*, Research Council on Structural Connections, Chicago, IL: American Institute of Steel Construction.

[29] Steinhardt, O., Möhler, K., and Valtinat, G., 1969. *Versuche zur anwendung vorgespannter schrauben im stahlbau*. IV. Teil. Berichte des deutschen Ausschusses für Stahlbau, 25.

[30] AWS (1928). *Code for Fusion Welding and Gas Cutting in Building Construction*, New York City, NY: American Welding Society.

[31] ABAQUS, 2011. *ABAQUS/CAE User's Manual, Version 6.11*, Dassault Systemes Simulia Corp, Providence, RI.

[32] Fisher, J.W., Frank, K. H., Hirt, M. A., McNamee, B. M, 1970. *Effect of weldments on the fatigue strength of steel beams*, National Cooperative Highway Research Program Report 102, Fritz Engineering Laboratory, Lehigh University, Bethlehem, PA.

[33] Fisher, J.W., Albrecht, P. A., Yen, B. T., Klingereman, D. J., McNamee, B. M., 1974. *Fatigue Strength of steel beams with welded stiffeners and attachments*, National Cooperative Highway Research Program Report 147, Fritz Engineering Laboratory, Lehigh University, Bethlehem, PA.

[34] Fisher, J.W., Barthelemy, B.M., Mertz, D.R., Edinger, J.A.,1980. *Fatigue Behavior of full-scale welded bridge attachments*, National Cooperative Highway Research Program Report 227, Fritz Engineering Laboratory, Lehigh University, Bethlehem, PA.

[35] NI, 2018. *LabVIEW NXG 3.0 User Manual*, National Instruments, Austin, TX, https://www.ni.com/documentation/en/labview/3.0/manual/manual-overview/. Accessed 10 Dec. 2018.

[36] EN 1993-1-8, 2005. *(English): Eurocode 3: Design of Steel Structures – Part 1-8: Design of Joints*, The European Union per Regulation 305/2011, Directive 98/34/EC, Directive 2004/18/EC

[37] Dusicka, P. and Lewis, G., 2007. *Effect of fillers on steel girder field splice performance Year 1 progress report*, Research Council on Structural Connections, Department of Civil and Environmental Engineering, Portland State University, Portland, OR.

[38] Grondin, G., Jin, M., Josi, G., 2007. *Slip critical bolted connections – A reliability analysis for design at the ultimate limit state.* Report prepared for The American Institute of Steel Construction. Department of Civil & Environmental Engineering, University of Alberta, Edmonton, Alberta, Canada.

[39] Borello, D. J., Denavit, M.D., Jerome, F. H., 2009. *Behavior of Bolted Steel Slip-Critical Connections with fillers.* Report No. NSEL-017, Newmark Structural Engineering Lab, Department of Civil and Environmental Engineering, University of Illinois at Urbana-Champaign, Urbana, IL.

VITA

Caleb W. Bennett

Candidate for the Degree of

Master of Science

Thesis: EVALUATING THE BEHAVIOR OF AXIAL LAP STEEL CONNECTIONS MADE IN COMBINATION OF SLIP-CRITICAL BOLTS AND LONGITUDINAL FILLET WELDS UNDER TENSION AND FATIGUE

Major Field: Civil Engineering

Biographical:

Education:

Completed the requirements for the Master of Science in Civil Engineering at Oklahoma State University, Stillwater, Oklahoma in July, 2021.

Completed the requirements for the Bachelor of Science in Civil Engineering at Oklahoma State University, Stillwater, Oklahoma in May, 2019.

Experience:

Graduate Research Assistant, School of Civil and Environmental Engineering, Oklahoma State University, Stillwater, Oklahoma, August 2019 – July 2021

Structural Engineering Intern, Wallace Engineering, Oklahoma City, Oklahoma, May 2019 – August 2019

Undergraduate Research Assistant, School of Civil and Environmental Engineering, Oklahoma State University, Stillwater, Oklahoma, February 2018 – May 2018 and August 2019 – May 2019

Professional Memberships:

Chi Epsilon – Civil Engineering Honor Society, 2017